

THESIS / THÈSE

MASTER EN BIOCHIMIE ET BIOLOGIE MOLÉCULAIRE ET CELLULAIRE

Étude du système de chimiotaxie négative au cuivre de *Caulobacter crescentus*

Cherry, Pauline

Award date:
2018

Awarding institution:
Universite de Namur

[Link to publication](#)

General rights

Copyright and moral rights for the publications made accessible in the public portal are retained by the authors and/or other copyright owners and it is a condition of accessing publications that users recognise and abide by the legal requirements associated with these rights.

- Users may download and print one copy of any publication from the public portal for the purpose of private study or research.
- You may not further distribute the material or use it for any profit-making activity or commercial gain
- You may freely distribute the URL identifying the publication in the public portal ?

Take down policy

If you believe that this document breaches copyright please contact us providing details, and we will remove access to the work immediately and investigate your claim.



Faculté des Sciences

**STUDY OF THE *CAULOBACTER CRESCENTUS* COPPPER-INDUCED NEGATIVE
CHEMOTAXIS SYSTEM**

**Mémoire présenté pour l'obtention
du grade académique de master 120 en biochimie et biologie moléculaire et cellulaire**

Pauline CHERRY

Janvier 2018

Université de Namur
FACULTE DES SCIENCES
Secrétariat du Département de Biologie
Rue de Bruxelles 61 - 5000 NAMUR
Téléphone: + 32(0)81.72.44.18 - Téléfax: + 32(0)81.72.44.20
E-mail: joelle.jonet@unamur.be - <http://www.unamur.be>

Étude du système de chimiotaxie négative au cuivre de *Caulobacter crescentus*

CHERRY Pauline

Résumé

La chimiotaxie fournit aux bactéries la capacité de sentir leur environnement et de s'adapter aux variations en nageant vers un nutriment (attractant) ou en fuyant un composé toxique (répulsif). Il a été montré précédemment que la cellule flagellée de *Caulobacter crescentus* peut fuir un stress au cuivre. Comme les mécanismes moléculaires sous-jacents de ce processus ne sont toujours pas connus, le but de ce projet sera de caractériser la réponse chimiotactique de *C. crescentus* et plus précisément, le rôle des 2 histidine kinases CheA prédites chez *C. crescentus* au sein d'un stress au Cu.

La prédiction de la structure protéique suggère que CheAI possède une structure classique tandis que CheAII possède des caractéristiques uniques telles que l'absence de domaine P2 ou bien la présence de 2 domaines P5. Les gènes encodant ces 2 protéines font partie de 2 opérons de chimiotaxie distincts : alors l'opéron *cheAI* est conservé chez de nombreuses Protéobactéries, l'organisation de l'opéron *cheAII* semble restreinte à certaines α -protéobactéries. Afin de fournir des preuves expérimentales aux observations *in silico*, des souches délétées des gènes *cheAI* et *cheAII* ont été construites et caractérisées. Deux techniques différentes de caractérisation de la chimiotaxie ont montré un rôle potentiel de CheAI dans la chimiotaxie puisqu'une délétion de ce gène entraîne une suppression du phénotype chimiotactique, ce qui n'est pas le cas si *cheAII* est délété. D'un autre côté, l'expression génique de *cheAI* et *cheAII* a été quantifiée par RT-qPCR. Il s'avère que *cheAI* est induit dans les cellules prédivisionnelles tandis que l'induction de *cheAII* a lieu également dans les cellules pédonculées, qui ne sont pas chimiotactique. Le rôle de CheAII dans la chimiotaxie ou dans un autre processus développemental reste flou.

Le deuxième aspect de cette étude vise l'identification d'autres acteurs impliqués dans la réponse chimiotactique au Cu. Dès lors, une stratégie de génétique sans *a priori* a été amorcée avec le développement d'un test de chimiotaxie adapté au screening de mutants transpositionnels dont la chimiotaxie au Cu est altérée. Vingt-trois mutants ont été isolés et caractérisés *via* notamment mesure de leur croissance, de leur phénotype de chimiotaxie au Cu ou encore par identification du site d'insertion du transposon.

Mémoire de master 120 en biochimie et biologie moléculaire et cellulaire

Janvier 2018

Promoteur: J.-Y. Matroule

Université de Namur
FACULTE DES SCIENCES
Secrétariat du Département de Biologie
Rue de Bruxelles 61 - 5000 NAMUR
Téléphone: + 32(0)81.72.44.18 - Téléfax: + 32(0)81.72.44.20
E-mail: joelle.jonet@unamur.be - <http://www.unamur.be>

Study of the *Caulobacter crescentus* copper-induced chemotaxis system

CHERRY Pauline

Summary

Bacterial chemotaxis provides the capacity to sense the environment and to adapt to external variations by swimming toward a nutrient (the attractant) or fleeing a toxic compound (the repellent). It was previously shown in the lab that *Caulobacter crescentus* swarmer cell swims away from a Cu stress. As the molecular mechanism(s) underlying this process is/are still unknown, the aim of this project will be the characterization of the *C. crescentus* chemotaxis response and more precisely the role of the 2 predicted *C. crescentus* CheA histidine kinase homologues in Cu stress environment.

Structure prediction suggests a CheAI typical structure while CheAII exhibits unique features such as the absence of any P2 domain and 2 P5 domains. CheAI- and CheAII-encoding genes are part of 2 distinct chemotaxis operons: while the *cheAI* operon is conserved in many Proteobacteria, the *cheAII* operon-like organization appears to be restricted to some α proteobacteria. In order to provide experimental confirmation of the *in silico* predictions, *cheAI/II* knockout strain were constructed and characterized. Two different chemotaxis techniques highlighted a potential role of CheAI in chemotaxis as deletion of this gene resulted in no chemotaxis, opposed to *cheAII* deletion. On the other side, gene expression of *cheAI* and *cheAII* was monitored through RT-qPCR. *cheAI* is expressed in predivisional cells while *cheAII* is induced in predivisional cells but also in stalked cells, which are not chemotactic. The role of CheAII in chemotaxis or in other developmental processes is still unclear.

The second aspect of this study aims at identifying the actors involved in Cu chemotaxis response. Therefore, a forward genetics strategy was initiated with the development of a chemotaxis assay adapted to the screening of transposition mutants impaired in the Cu-induced negative chemotaxis. Twenty-three mutants were retrieved and characterized by monitoring their growth, measuring Cu-induced chemotaxis as well as identifying transposon insertion site.

Mémoire de master 120 en biochimie et biologie moléculaire et cellulaire

Janvier 2018

Promoteur: J.-Y. Matroule

Acknowledgements

J'aimerais tout d'abord remercier Jean-Yves Matroule, mon promoteur, de m'avoir offert la possibilité de réaliser mon mémoire au sein de son équipe ainsi que pour son optimisme et ses encouragements, notamment lorsqu'aucune PCR ne fonctionnait.

Merci Gwen, mon encadrante qui m'a non seulement transmis sa passion pour la science et la chimiotaxie mais aussi pour sa patience pour mes nombreuses questions ou des manips qui ne fonctionnent pas du premier coup (ni même du 5^{ème}). Merci d'avoir partagé des moments de joie (oh un mutant *cheAI* !), des moments d'angoisse (où sont passé les mutants *cheAI* ?) ou tout simplement, de longues discussions qui concernent de près ou de loin la science.

Je remercie d'ores et déjà les membres du jury, Élise Durmortier, Victoria Vassen, Jérôme Coppine et Régis Hallet, pour l'attention qu'ils ont porté et porteront à ce projet ainsi que le temps consacré à la lecture de ce mémoire.

Un tout grand merci membres de la BEAR team, anciens et présents, Eme, Seb et Françoise pour leur bonne humeur, leurs conseils mais aussi leur aide. Merci couz' pour les longues discussions labo/manips/ragots pendant les réunions de famille, je continue sur tes traces ! Seb, merci pour ton aide bioinformatique et pour mes manips quand Gwen se cachait, merci pour ta curiosité quand je testais de nouvelles choses (il est 16h non ?). Merci Françoise pour ta gentillesse et toutes les boites de crible que tu mettais de côté pour moi. Mis à part ça, à quand une sortie BEAR Urbex ?

Merci à tous les membres de l'URBM de garder une ambiance agréable et une convivialité au sein du labo ainsi qu'aux membres de GeMo qui, tous les vendredis, organisent une beer hour comme il se doit (il est 16h ! Seb ? Gwen ?).

Je voudrais également remercier tous les autres mémos qui se sont embarqués avec moi dans l'aventure d'un mémoire en URBM. Merci Caro de m'avoir accompagnée dans les PCR qui ne fonctionnent pas. Béa, garde ta bonne humeur et ton accent espagnol, je rigole tellement (jui-yeah) ! Merci Audrey et Sarah pour les longues conversations qu'on a pu avoir à la place de travailler (Oh, un méga trou !). Merci Thomas et Elie pour les discussions Caulo et autres ragots.

Enfin, j'aimerais remercier ma maman et mon frère qui ont réussi à me supporter quand rien ne fonctionnait ou quand, pendant les vacances, le réveil sonne. Merci de m'avoir supportée pendant ces 5 longues années d'études qui sont finalement, très positives grâce à votre soutien. Pour terminer, j'aimerais remercier Pierre qui m'a accompagnée pendant toutes mes études et qui m'a prouvé que quand on veut, on peut. Merci d'avoir cru en moi, d'avoir enduré tous mes coups de gueule ou tous mes moments de folie qui n'ont très certainement pas diminué ton nombre de cheveux blancs.

« Pas de patience, pas de science »

Jean-Pierre Jarroux

Table of contents

Introduction	6
I. Bacterial adaptive responses to stress	6
II. Copper	12
III. <i>Caulobacter crescentus</i>	13
Objectives	15
Results and discussion.....	16
I. <i>In silico</i> characterization of <i>cheA</i> genes and protein.....	16
II. Characterization of single and double <i>cheA</i> KO mutants.....	18
III. Expression of <i>cheA</i> genes	19
IV. Isolation and characterization of chemotaxis mutants.....	21
Conclusion and perspectives	23
Experimental procedures	24
I. Strains, plasmids and growth conditions.....	24
II. Growth curve measurements	25
III. DNA quantification by flow cytometry.....	25
IV. Gene expression quantification	25
V. Live chemotaxis imaging.....	27
VI. Chemotaxis mutant screening.....	27
Bibliography	29
Annexes	34

Introduction

I. Bacterial adaptive responses to stress

Bacteria is a large domain of life that consists of prokaryotic microorganisms. These microorganisms are usually unicellular and can be found in every biotope present on Earth. Bacteria can also colonize and inhabit extreme environments such as polluted soils, deserts or hot springs. Because the composition of an environment can fluctuate, all living organisms are subject to changes that can generate stressful conditions such as nutrient deprivation or exposure to toxic compounds. Bacteria can face these stresses through an adaptive response to cope with the new environmental conditions. Different adaptation strategies can be found depending on the bacterial organism and some of them are described below.

In the environment, most of the bacteria live within biofilms. These structures are resulting from the association of one or several bacterial species, embedded in a specific matrix. The components of the matrix, called extracellular polymeric substances, are synthesized by the bacteria. The biofilm favors cellular processes such as horizontal gene transfer or tolerance to antimicrobial substances. The biofilm matrix can considerably reduce the antimicrobial activity of some toxic substances (Flemming et al. 2016). For example, the γ -proteobacteria *Erwinia amylovora*'s biofilm matrix complexes copper ions to protect the bacteria from high copper concentrations (Ordax et al. 2010).

Another strategy to face a changing environment is cellular differentiation. Filamentous *Anabaena* sp. cyanobacterium is photosynthetic and can fix atmospheric nitrogen. Nevertheless, these 2 metabolisms are incompatible as the nitrogen-fixing nitrogenase is inactivated by the oxygen produced during photosynthesis. The mechanism developed by *Anabaena* consists in a spatial and temporal separation of these processes by cellular differentiation. Upon nitrogen starvation, 10 % of vegetative cells differentiate into a heterocyst, which switches its metabolism from photosynthesis to N₂ fixation. Once incorporated in amino acids, fixed nitrogen is distributed to neighboring cells, which provide carbon sources to the heterocyst (Kumar et al. 2010).

Some bacteria developed the ability to form spores such as the Gram-positive bacteria *Clostridium difficile* and *Bacillus subtilis*. Moreover, the Gram-negative bacterium *Myxococcus xanthus* displays a complex cell cycle that also involves the spore formation. This distinct cell type formation is mediated either by starvation, cell death or quorum sensing. It involves metabolism, gene expression and phenotypic changes. Once the spore is formed, this metabolically dormant cell is able to survive to different environmental stresses such as desiccation, extreme temperatures, immune system or disinfectants. When the environment becomes favorable, the spore germinates and leads to the formation of a fully functional bacteria, able to initiate a new cell cycle (Zusman et al. 2007; Higgins & Dworkin 2012; Paredes-Sabja et al. 2014).

The 3 previous described adaptation strategies (i.e. biofilms, cellular differentiation and spore formation) are time- and resource-consuming and they depend on the bacteria capacity to develop different cellular structures. On the opposite, the chemotaxis system drives bacteria to nutrients (positive chemotaxis) or away from toxic compounds (negative chemotaxis) and relies on bacterial motility. This system will be discussed in further details in the subsequent section.

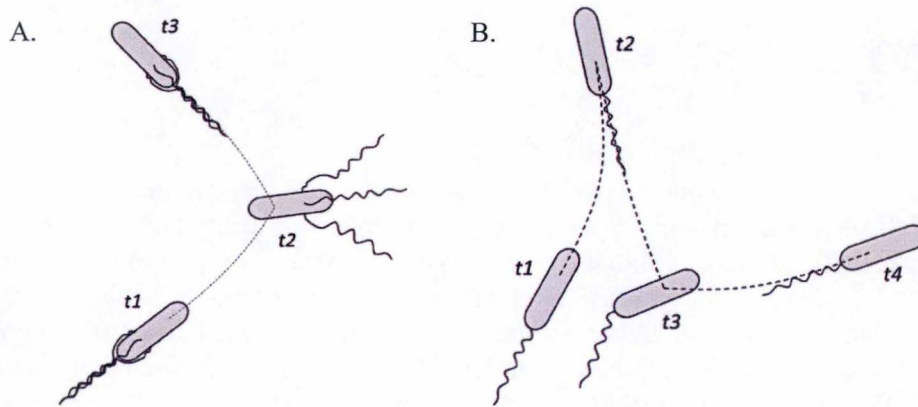


Figure 1. Motility patterns. **A.** Motility pattern of multiflagellated bacteria. Forward runs are characterized by CCW (counter-clockwise) rotation of the flagella (*t1*). The change of one or more flagella from CCW to CW (clockwise) rotation leads to the tumbling of the bacteria and to a new swimming direction (*t2*). Following reorientation, bacterium goes forward again (*t3*). **B.** Motility pattern of uniflagellated bacteria. The swimming pattern is characterized by a succession of forward and backward runs when flagellum rotates CW (*t1*) and CCW (*t2*) respectively. Backward runs creates tension within the flagellum (*t3*), leading to a new bacterium orientation for the next forward run (*t4*).

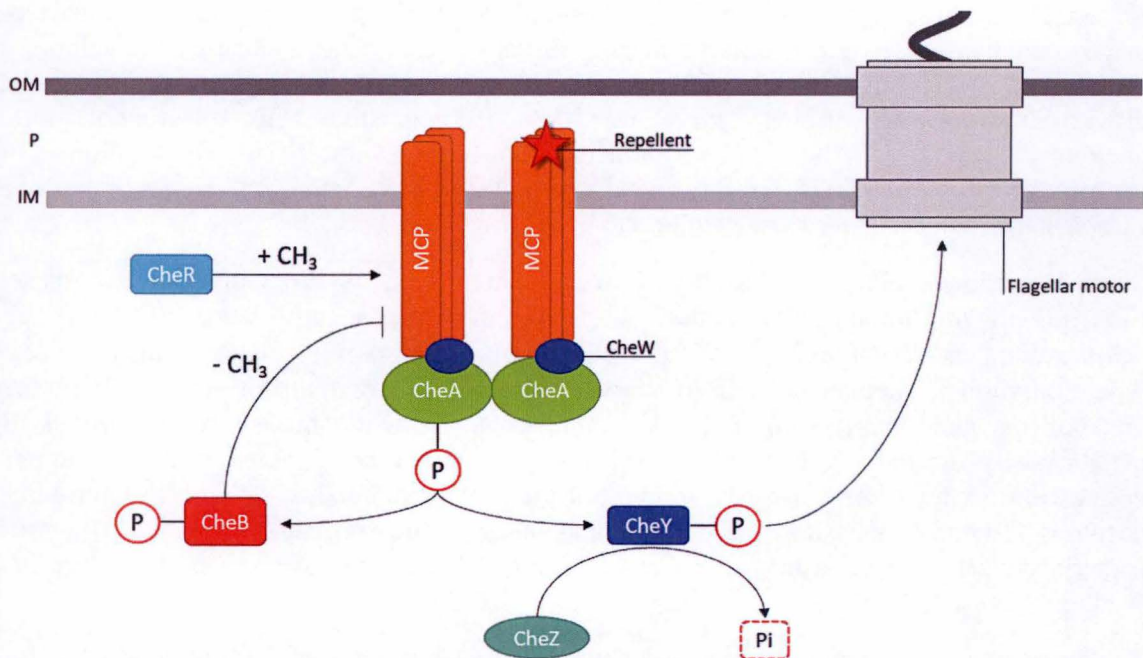


Figure 2. *Escherichia coli* chemotaxis system. Upon the binding of a repellent to a chemoreceptor (MCP), conformational changes occur and lead to the activation, resulting to the autophosphorylation of the histidine kinase CheA, coupled to the MCP by CheW. CheA~P can transfer its phosphoryl group to 2 response regulators: CheY and CheB. CheY~P can interact with FliM, the flagellum-associated switch protein, which results in the modification of motor switching frequency. To terminate the signal, the phosphatase CheZ can dephosphorylate CheY~P. On the contrary, CheB-P can remove methyl groups from MCPs regulatory domain to compensate CheR methyltransferase effects. CheB and CheR are part of the adaptive system to reset the MCP sensitivity to ligand.

A. Chemotaxis system

Bacterial chemotaxis is the biased movement of a motile bacteria toward attractants such as nutrients or away from repellent (i.e. toxic compounds). In homogeneous environments such as laboratory medium, bacterial movements are random. *Escherichia coli* movements and direction changes are based on the “run-and-tumble” model (Fig. 1A). In this model, the rotation change from counter-clockwise (CCW) to clockwise (CW) of one or several flagella results in a tumble of the bacterium, leading to a reorientation (70° angle in *E. coli*) of the cell. Upon reorientation, the bacterium resumes a straight movement in a new direction (Taktikos et al. 2013). Some uniflagellar bacteria, such as *Vibrio alginolyticus* or *Caulobacter crescentus* use the “run-reverse-flick” model (Fig. 1B). Their swimming pattern is cyclic with an alternation of forward and backward runs. The forward run is mediated by the flagellum pushing the cell (CW rotation), the backward run by the flagellum pulling the bacteria (CCW rotation). The backward movement creates a tension within the flagellum, leading to a modification in the orientation of the bacteria, therefore creating a new swimming direction (Taktikos et al. 2013; Son et al. 2013; Morse et al. 2015).

These motility patterns can be biased by the chemotaxis system. In the presence of a nutrient, the bacteria decrease the frequency of reorientations in order to swim longer in the same direction. On the opposite, repellents induce an increase of this frequency to flee this stress (Wadhams & Armitage 2004; Taktikos et al. 2013; Son et al. 2013). Chemotaxis has been extensively studied in *E. coli* but it seems that the signaling pathway underlying chemotaxis is conserved among all chemotactic bacteria and archaea. Moreover, it has been shown that bacteria living in a complex environment are more susceptible to use complex chemotaxis system as well as multiple chemosensory pathways (Lacal et al. 2010; Wuichet & Zhulin 2010).

In *E. coli*, the first proteins involved in chemotaxis are the MCPs (methyl-accepting chemotaxis protein). These proteins act as sensors and may bind multiple compounds. When activated by the binding of a repellent ligand, MCPs stimulate the autophosphorylation of the associated CheA histidine kinase (CheA~P). CheA binding to the MCP cytoplasmic domain relies on the CheW adaptor. Once phosphorylated, CheA~P transfers its phosphate to the CheY response regulator (CheY~P), which in turn binds the flagellum-associated switch protein FliM. This CheY~P-FliM interaction increases the number of rotation changes of the flagellum. To terminate the signal, the CheZ phosphatase dephosphorylates CheY~P. On the other side, the methyltransferase CheR and the methylesterase CheB mediate the MCP adaption to the signal (Fig. 2). Each of these actors will be described in the following dedicated sections.

1. Signal sensing

In the chemotaxis signaling pathway, the signal is sensed by chemoreceptor arrays. These supramolecular structures comprise MCP chemoreceptors, CheA histidine kinases and CheW coupling proteins. The structures can either be inserted into the inner membrane or be cytoplasmic. The array localization depends on the MCPs solubility which is itself based on its cognate ligand (Salah Ud-Din & Roujeinikova 2017).

Independently of the localization, the array structure is conserved and is characterized by a hexagonal organization. The protein assembly underlying this organization is based on the interaction between MCPs, CheA and CheW. The minimal unit required for signal transduction is composed of 2 MCP trimers-of-dimers interacting with 2 CheW proteins and 1 dimeric CheA in a ring structure (Fig. 3A and B). This organization provides sensitivity, stability, dynamic range of activation and a feedback control of the chemotaxis system. In chemotaxis arrays, this arrangement is repeated and can include thousands of proteins (Fig. 3C) (Briegel et al. 2012; Jones & Armitage 2015; Parkinson et al. 2015). In the case of cytoplasmic arrays, MCPs form

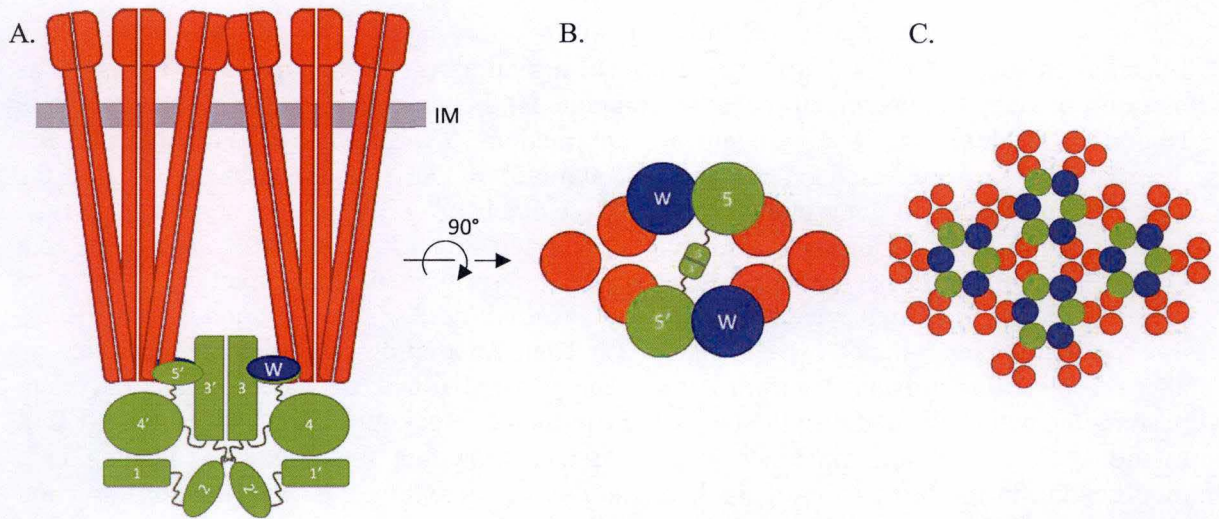


Figure 3. Chemotaxis array organization. **A.** MCP are forming trimers-of-dimers and, at the tip of the cytoplasmic signalling domain, CheW and CheA are bound. The minimal functional subunit is made of 6 MCP dimers, 2 CheW and 1 CheA dimer. **B.** CheW and P5 domains from CheA are also interacting, leading to hexagonal ring structure, **(C.)** which is the organization base of chemosensory cluster that contains hundreds of proteins.

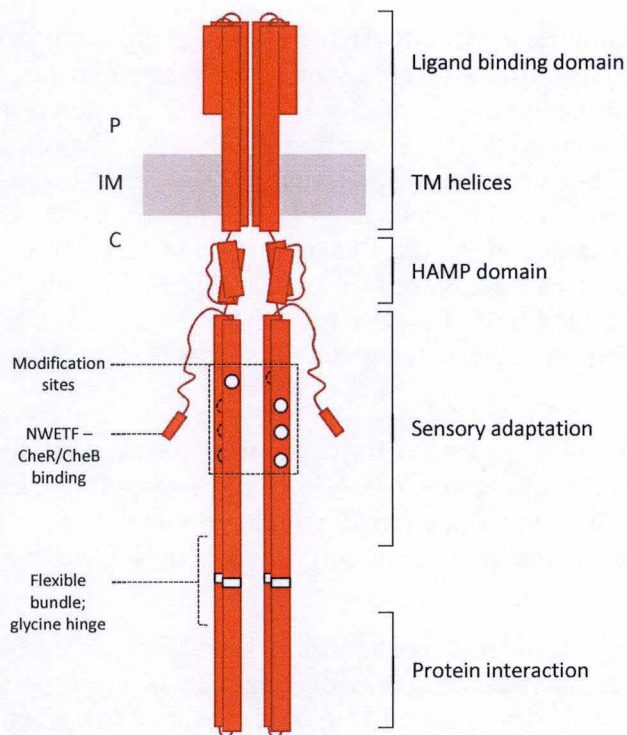


Figure 4. MCP dimer structure. The ligand binding domain can bind free diffusing compounds as well as binding proteins. Binding induces conformational changes transmitted to the HAMP domain and to the tip of the dimer, where CheA and CheW are bound. CheB and CheR interact with the C-terminus motif NWETF and modify the 4 residues that are represented in white.

a two-layer structure that is comprised between 2 CheA-CheW plates (Salah Ud-Din & Roujeinikova 2017).

Clusters of chemosensory arrays are preferentially localized at the cell poles, regardless of their solubility (Gestwicki et al. 2000). Multiple array positioning patterns have been identified in different organisms. *E. coli* displays a large array at one cell pole in addition to smaller clusters inserted in lateral membranes. On the contrary, *Rhodobacter sphaeroides* arrays are distinctly positioned within the cells, depending on their solubility. Upon division, the challenge is to furnish each motile daughter cell with at least one chemotaxis array. To this end, new arrays are synthesized and, are preferentially segregated to each pole of the dividing cell through different mechanisms. It ensures that each daughter cell will inherit an array at its old pole (Jones & Armitage 2015; Alvarado et al. 2017).

a. Methyl-accepting chemotaxis proteins (MCP)

The MCPs are receptors that can bind multiple ligands. The number of MCP genes goes from 1 in *Mezorhizobium loti*, to 5 in *E. coli*, and 89 in *Azospirillum* sp. B510 (Wadhams & Armitage 2004; Salah Ud-Din & Roujeinikova 2017). It has been observed that the number of MCP genes can be correlated with the complexity of the organism lifestyle or with a high metabolic diversity (Lacal et al. 2010).

The structures of the MCPs Tar and Tsr from *E. coli* have been extensively studied and are used as models for other MCPs. As previously described, these proteins form dimers that are functional upon the formation of trimers. MCPs are composed of 3 domains: a periplasmic ligand-binding domain, a transmembrane domain and a cytoplasmic signaling domain that comprises a HAMP domain (present in histidine kinases, adenylyl cyclases, methyl-accepting proteins and phosphatases) (Fig. 4). The ligand-binding domain can bind free molecules as well as ligand-binding proteins (Wadhams & Armitage 2004; Parkinson et al. 2015).

Upon ligand binding, the ligand-binding domain undergoes conformational changes that are transmitted to the HAMP domain. In the MCP trimer-of-dimers form, this conformational change has an impact on the signaling domain which can, in turn, stimulate or inhibit the kinase activity of CheA (Khursigara et al. 2008). In absence of the HAMP domain, the signal transduction is impaired (Lai & Parkinson 2014).

Compared to the ligand-binding domain, the cytoplasmic signaling domain is highly conserved throughout chemotactic prokaryotes. It consists of a sensory adaptation subdomain and a protein interaction domain, both linked by a flexible bundle of glycine hinge (Parkinson et al. 2015). The sensory adaptation subdomain contains several crucial residues within a consensus sequence that can be methylated by CheR or demethylated by CheB, which bind the conserved C-terminus motif NWTEF (Parkinson et al. 2015; Salah Ud-Din & Roujeinikova 2017). The adaptive system will be described in the subsequent dedicated section. On the opposite, the interaction subdomain directly interacts with CheA and CheW. A hairpin in the MCPs is responsible for CheA kinase activation through conformational changes. The residues composing this hairpin have the highest amino acid conservation among MCPs. Following HAMP conformation state, the hairpin can be found in 2 conformations that either activate or inhibit CheA activity (Parkinson et al. 2015; Salah Ud-Din & Roujeinikova 2017).

Moreover, MCPs cytoplasmic domain seems to be involved in membrane insertion. It has been firstly shown in *C. crescentus* that the carboxyl end of the protein is responsible for its targeting into the inner membrane (Alley et al. 1992). The Sec machinery found in *E. coli* could interact with this end in order to insert the MCP into the membrane (Shiomi et al. 2006).

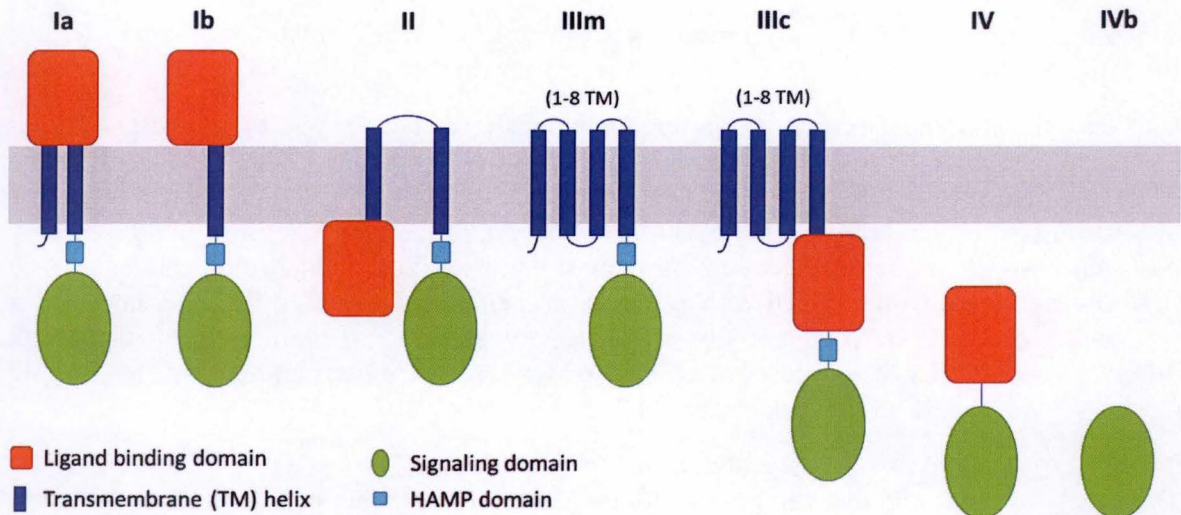


Figure 5. Classification of MCP into 7 families based on membrane domain topology and ligand binding domain (adapted from Lacal et al. 2010).

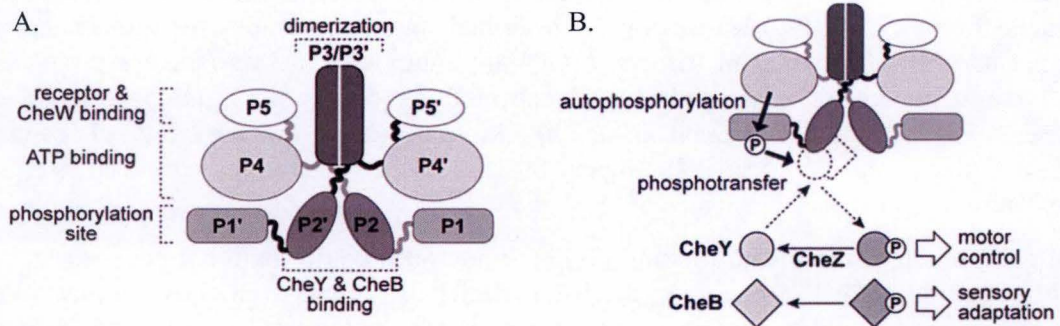


Figure 6. Domain structure and signalling transduction of *E. coli* CheA. **A.** Functional CheA homodimer with domain function. One subunit has its domains linkers in black, the second one linkers are in grey. **B.** CheA phosphorylation catalysis. The P4 domain phosphorylates P1 domain which transfers its phosphoryl group onto CheY and CheB docked on P2 domain (Nishiyama et al. 2014).

The previously described protein structure is the typical structure of 4 out of the 5 *E. coli* MCPs. The chemotaxis pathway diversity also applies to the MCP structures and these are a variation on a theme. In 2010, Lical and colleagues analyzed more than 350 available sequences of MCPs and classified them into seven topology families (Ia, Ib, II, III_m, III_c, IV_a and IV_b) (Fig. 5) (Lical et al. 2010). The topology I is the predominant structure of MCPs in prokaryotes while the classes II and IV are usually involved in aerotaxis or in sensing the redox status of the cytoplasm. The archaeon *Halobacterium salinarum* class III MCP is a phototaxis receptor (Salah Ud-Din & Roujeinikova 2017). High diversity can also be found in the ligand-binding domain. Among chemotactic organisms, there are numerous structure families but, even within a family, the sequences are highly divergent. It could suggest that only the structure is important, compared to the sequence. On the other side, convergence can also lead 2 distinct MCPs to bind the same ligand through completely different mechanisms (Ortega et al. 2017).

b. *CheW*

CheW is a coupling protein that interacts with the MCP C-terminal region and one domain of CheA (P5 domain), enabling coupling of CheA to MCP. The structure of CheW from *E. coli* is solved and this protein seems to be a paralog the P5 domain from CheA. This homology is thought to be the basis of CheA-CheW interaction (Bhatnagar et al. 2010). Notwithstanding the absence of catalytic activity, the scaffolding role of this protein is significant as a deletion completely inhibits signal transduction and, therefore, chemotaxis (Li et al. 2007; Kentner & Sourjik 2009). It should be noted that this protein is highly conserved among chemotactic prokaryotes, as well as MCPs, CheA, CheR and CheB. These proteins are thought to form the chemotaxis signaling core (Wuichet & Zhulin 2010). All these observations suggest that CheW has an important role in chemotaxis, at least in chemosensory array scaffolding and in signal transduction.

c. *CheA*

The third element of the chemoreceptor array is the histidine kinase CheA. This protein transmits the MCPs signal to its response regulators and, eventually, to the flagellar motor. The functional histidine kinase is a dimer composed of 78 kDa monomers. Both subunits have five distinct domains with different functions (Fig. 6). The P1 domain is an HPt (histidine phosphotransfer) domain which contains a histidine, in position 48 in *E. coli*, that can be transphosphorylated. This transphosphorylation is mediated by the P4 domain that binds ATP. While the P3 domain is responsible for dimerization, the P2 and P5 domains interact with different chemotaxis proteins: CheY and CheB or CheW and MCP, respectively (Bilwes et al. 1999; Mo et al. 2012; Nishiyama et al. 2014).

The activation of CheA by MCPs depends on conformational states. When CheA is in the active state, P1 and P4 are tightly bound and properly aligned for the phosphorylation reaction. The autophosphorylation relies on interactions between residues from the P4 domain and some residues of the P3-P4 linker with residues surrounding His48 from P1 domain (Nishiyama et al. 2014; Wang et al. 2014). On the contrary, the inactive state is characterized by loosely associated P1 and P4 domains (Levit et al. 1999; Nishiyama et al. 2014). These allosteric changes are triggered by MCP conformational changes induced by the binding of a ligand. The triple interaction between the MCP, CheW and CheA seems to be important for the signal transduction and, therefore, the activation of CheA (Schulmeister et al. 2008; Parkinson et al. 2015). When an attractant binds to a MCP, the conformational changes lead to the kinase-off state and to a decrease of tumbling events, maintaining the bacteria unidirectional movement. In contrast, the binding of a repellent leads to the kinase-on state of CheA which results in an increase of tumbles and, in turn, in a direction change.

Like other histidine kinases involved in two-component signal transduction systems, CheA~P interacts with response regulators (RRs). In *E. coli*, CheA~P binds and phosphorylates a conserved aspartate residue present in 2 proteins, the RR CheY and the methylesterase CheB (Hess et al. 1988). Notwithstanding the specific interaction between P1 domain and CheY, the P2 domain increases this specific binding and provides RRs docking to CheA (Mo et al. 2012). Moreover, this domain enhances of CheA phosphorylation rate by increasing the local concentration of CheY and CheB (Jahreis et al. 2004; Mo et al. 2012). Nonetheless, this domain is not essential for the histidine kinase activity (McEvoy et al. 1996). Once phosphorylated, the RRs are active and can interact with other proteins. The CheB~P methylesterase is responsible for the adaption of the MCPs sensitivity to their ligand. This RR is part of the adaptive system alongside the CheR methyltransferase. On the other side, the CheY~P RR can interact with the flagellar motor and modify the frequency of tumbling events. Both RRs will be discussed later.

2. Propagation and termination of the signal

a. *CheY*

Upon phosphorylation of the conserved Asp57 in *E. coli*, active CheY~P interacts with the flagellar protein FliM (Bourret et al. 1990). The phosphorylation induces CheY conformational changes, resulting in the dissociation from CheA~P and in a specific interaction with the FliM C-terminus (Bren & Eisenbach 1998). In *E. coli*, this interaction promotes a clockwise rotation of the flagellum and leads to tumbling of bacteria and to a new swimming direction.

CheY can also be acetylated on 6 lysine residues, which may interfere with the chemotaxis signaling. The acetylation can be catalyzed either by CheY itself or by an unknown acetyltransferase, using an acetyl-CoA as a donor. Moreover, acetylation and phosphorylation seem to exclude each other (Barak et al. 2006). Once acetylated, active CheY interacts with FliM, increasing the number of tumbling events (Barak & Eisenbach 2001). It has been shown that the acetylation is linked to the metabolic state of the cell and could be involved in repellent-induced chemotaxis only (Barak et al. 2006; Yan et al. 2008). In *E. coli*, the NAD⁺-dependent sirtuin CobB appears to be responsible for CheY deacetylation (Li et al. 2010). CheY phosphorylation and acetylation could differently control the pool of CheY proteins that can participate in chemotaxis signaling, in relation with the metabolic state of the bacteria (Liarzi et al. 2010).

b. *CheZ*

To terminate the signal, CheY~P needs to be dephosphorylated. The intrinsic phosphatase activity of CheY~P sets the half-life of CheY~P to about 20 seconds (Wadhams & Armitage 2004). In *E. coli*, the presence of the phosphatase CheZ decreases CheY~P half-life to 200 milliseconds, which allows temporal sensing required by the chemotaxis (Hess et al. 1988). In presence of CheY~P, CheZ forms a functional dimer, where the CheZ Gln147 is essential for the catalytic activity (Zhao et al. 2002).

3. Adaptive system

In heterogeneous environments, it is crucial for bacteria to sense small changes in attractant concentrations or to return to the pre-stimulus ligand sensitivity. As the size of the bacteria does not allow spatial comparison, the adaption is based on time. Every 3 to 4 seconds, the bacteria reset its sensitivity to ligand and is able to compare past and present concentrations in order to find the best environmental niche (Segall et al. 1986; Meir et al. 2010). The adaptive system is based on a negative feedback loop, depending on methylation and demethylation of MCP by two proteins: the CheR methyltransferase and the CheB methylesterase (Weis & Koshland 1988; Barkai & Leibler 1997). This robust system seems to be crucial in chemotaxis since these 2 proteins are present in more than 90 % of genomes containing chemotaxis components (Barkai & Leibler 1997; Wuichet & Zhulin 2010).

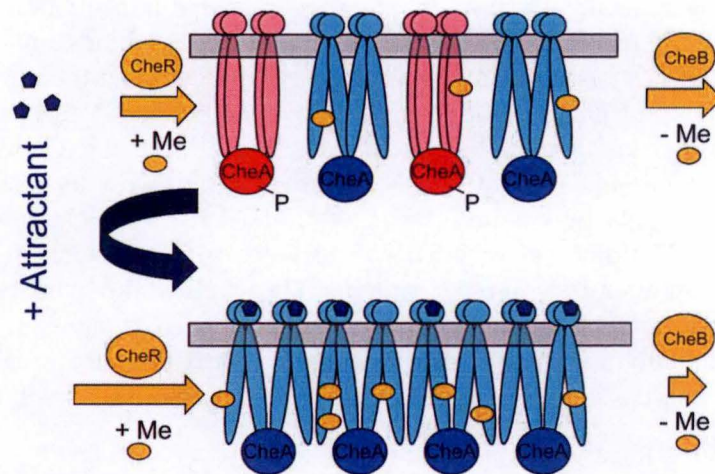


Figure 7. Adaptation of MCP in presence of an attractant. In basal conditions (*top*), the number of activated MCPs remains fixed by methylation and demethylation mediated by methylesterase CheB and methyltransferase CheR. Upon the addition of an attractant (*bottom*), MCPs turn inactive as well as CheA and only CheR remains active. CheR adds methyl groups, which increase MCP sensitivity to ligands (Meir et al. 2010).

In absence of any attractant, the CheR methyltransferase is constitutively activated and catalyzes the glutamyl methylation on inactive MCP. This reaction leads to the increase of methylated residues that have an effect on HAMP conformation, which increases the ability of MCP to activate CheA (Parkinson et al. 2015). On the other side, some MCPs are activated as well as CheA~P that can phosphorylate the methylesterase CheB, thereby leading to a 100 fold increase of its activity. This negative feedback loop sets the MCP sensitivity to a pre-stimulus state (Fig. 7). Upon the binding of an attractant, MCPs are inactivated and CheB is no more phosphorylated, resulting in only active CheR. The addition of methyl groups is a second negative feedback loop that allows the MCP adaptation to the current concentration of the ligand (Fig. 7) (Wadhams & Armitage 2004; Parkinson et al. 2015).

The modification and the adaptation of a chemoreceptor depend on interacting proteins, which are themselves based on the MCP activity state (Barkai & Leibler 1997). *In vivo*, MCPs are present in clusters and, in these arrays, not all MCPs bind a ligand. When CheR or CheB~P is tethered to one MCP, the protein can interact with 5 to 7 receptors that can be subsequently methylated or demethylated. These multiple interactions allow a precise adaptation of the chemotaxis system since it increases the extent of methylation levels from 8 levels for a single homodimer, up to 48 for 6 homodimers (Endres & Wingreen 2006).

In *E. coli*, it has been shown that, in absence of any functional CheR and CheB proteins, an adaptation of the chemotaxis system was still possible. In presence of a small pool of CheY~P, the flagellar motor increases its sensitivity by enhancing the number of FliM proteins. Therefore, the flagellum can sense small concentration changes of CheY~P. However, this adaptation is low and does not play a role in temporal gradient sensing. This system could be additional to methylation and it could allow a precise chemotaxis output (Yuan et al. 2012).

4. Alternative chemosensory pathways

The chemotaxis pathway from *E. coli* only displays 5 MCPs while most of the chemotactic organisms have at least 10 MCP-encoding genes in their genome and this number increases with the complexity of bacterial lifestyle. Moreover, some organisms have more than 1 chemotaxis systems (Wuichet & Zhulin 2010). In the next sections, different chemotaxis systems will be discussed as well as their implication in other processes than chemotaxis in 3 different organisms: *Rhodobacter sphaeroides*, *Myxococcus xanthus* and *Bacillus subtilis*.

a. Chemotaxis in *Rhodobacter sphaeroides*

The α -proteobacteria *R. sphaeroides* has a more complex chemotaxis system than *E. coli*. This bacteria exhibits an inner membrane chemoreceptor array and a cytoplasmic chemoreceptor array: (for a comprehensive review, see (Porter et al. 2008)). These 2 chemotaxis clusters are composed of specific chemotaxis proteins that are encoded from 3 distinct operons, leading to a chemotaxis protein redundancy. There are 13 MCPs, 4 CheA, 4 CheW, 6 CheY, 2 CheB and 3 CheR. CheA₂ has a structure similar to *E. coli* CheA and localizes to membrane arrays together with CheW₂ and CheW₃. This histidine kinase can phosphorylate all CheY and CheB proteins. On the contrary, CheA₃ and CheA₄ form an atypical histidine kinase. CheA₃ only contains P1 and P5 domains, while CheA₄ lacks domains P1 and P2. The unusual dimer resulting from these 2 subunits is found in association with the cytoplasmic array and only phosphorylates CheY₆ and CheB₂ (Porter & Armitage 2004). There is no chemotaxis phosphatase found in the genome of *R. sphaeroides* but it has been proposed that signal termination relies on a phosphate sink, where some CheY~P proteins do not interact with the flagellum but sequester phosphoryl groups instead (Porter et al. 2008).

In appearance, membrane and cytoplasmic clusters seem to be independent of each other since arrays contain non-interchangeable proteins and bind specific ligands. However, if one of the 2

arrays is deleted, chemotaxis is inhibited. It has been suggested that both clusters could communicate to induce an appropriate answer by comparing the concentration of an attractant to the metabolic state of the cell (Porter et al. 2008; Porter et al. 2011).

b. Chemotaxis in *Bacillus subtilis*

The Gram-positive bacterium *B. subtilis* is a ubiquitous organism present in soils. This complex environment led to the development of a unique chemotaxis pathway since *B. subtilis* carries 3 adaptation systems in its genome. Contrary to *E. coli*, the binding of an attractant leads to the activation of the MCP and CheA. Then, CheA~P phosphorylates CheY, CheB and a third RR, CheV which is made of a CheY and a CheW domains. The interaction between CheY~P and FliM induces smooth swimming, opposed to the increase of *E. coli* flagella tumbling rate. Moreover, there are no CheZ phosphatase and it is the flagellar FliY protein that dephosphorylates CheY~P. The adaptation of the chemotaxis system is mediated by 3 different systems: CheR and CheB, CheC and CheD, and CheV (Porter et al. 2011; Walukiewicz et al. 2014).

Like *E. coli*, CheR and CheB methylates and demethylates specific MCP residues to control ligand sensitivity. On the other side, CheC and CheD are part of a negative feedback loop that controls CheA activity. CheC is a weak phosphatase of CheY~P, while CheD is a receptor deamidase. Upon the binding of a ligand, CheA becomes active and phosphorylates CheY. The phosphorylated pool of this protein increases and stimulates the association of CheC and CheD. Once associated, CheC is able to dephosphorylate CheY~P at higher levels. When the number of CheY~P drops, CheC and CheD dissociate, CheD can remove amides groups from receptors, resulting in activation of CheA. Additionally, the activation of CheA is controlled by the CheV mediated-adaptation. Upon the phosphorylation of CheV by CheA, the phosphoryl group seems to inhibit the coupling of CheA to the receptors, inactivating signal transduction (Walukiewicz et al. 2014).

c. Chemotaxis in *Myxococcus xanthus*

M. xanthus is a δ -proteobacteria that can be found in soils. This bacterium undergoes a complex cell cycle that leads to the formation of fruiting bodies and spores. Despite the absence of a flagellum, *M. xanthus* glides on solid surfaces and can eventually revert its orientation. *M. xanthus* gliding motility speed is quite slow (2-4 μm per minute) compared to *E. coli* swimming speed (~50 μm per second). This speed seems to be incompatible with chemotaxis since it is based on temporal comparison. However, both positive and negative chemotaxis have been described in *M. xanthus* (Zusman et al. 2007).

The genome of *M. xanthus* contains 8 chemotaxis-like operons. While the role of each operon is not known, some seems to be implicated in chemotaxis or in the regulation of developmental genes. The *frz* operon is implicated in chemotaxis and contains homologs of *E. coli che* genes. The MCP FrzCD activates the autophosphorylation of FrzE, a hybrid histidine kinase (CheA-CheY). FrzA, a CheW-like protein, couples FrzCD and FrzE. The signal is transmitted through FrzZ (CheY) that ultimately mediates bacteria reversal (Zusman et al. 2007; Mercier & Mignot 2016). This chemotaxis system is notably involved in colonies movements during predation of other microbial species (Berleman et al. 2008). The third chemotaxis-like operon is involved in developmental timing and gene expression. This sensory pathway results in the activation of a transcriptional factor that activates gene expression involved in the development of *M. xanthus* (Zusman et al. 2007).

II. Copper

Metal ions are essential for bacteria as they are used as cofactors by metalloproteins. In the early stages of life, iron (Fe) was mainly used owing its solubility (Fe(II)) in a reduced

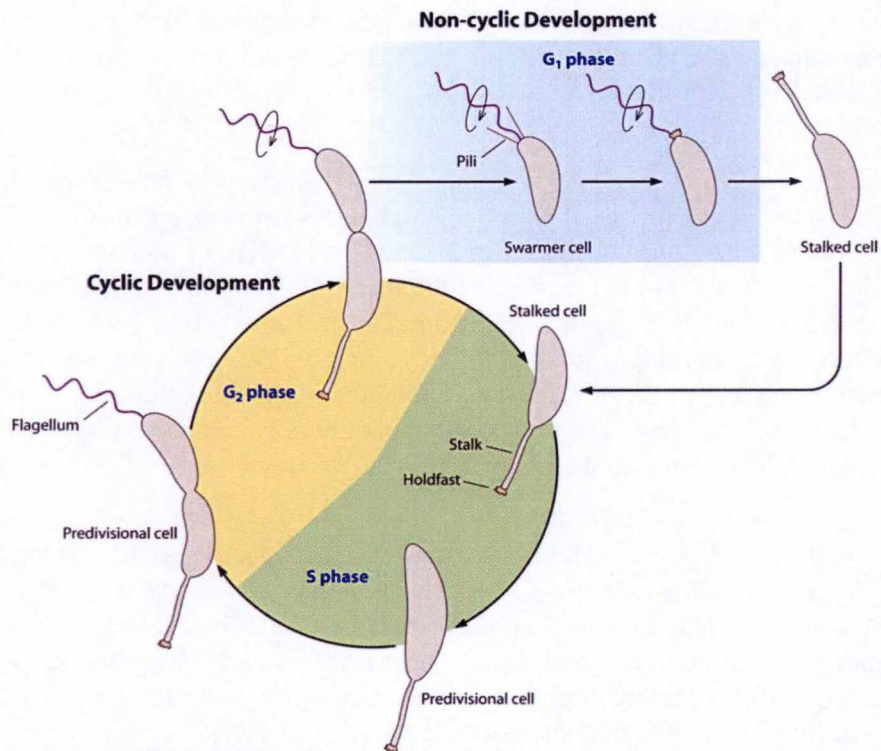


Figure 8. Cell cycle of *Caulobacter crescentus*. The non-cyclic development process concerns the swarmer cell differentiation into a stalked cell. Only this morphotype is able to replicate its chromosome and to initiate a cyclic development process. Upon division, the stalked cell become a predivisional cell with 2 different poles, each one referring to the future daughter cells. Upon division, the 2 daughter cells can undergo non-cyclic development (swarmer cell) or a new cyclic development (stalked cell) (Curtis and Brun 2010).

environment. The oxygen released by photosynthetic cyanobacteria led to the decrease of Fe bioavailability (insoluble Fe(III)) and the increase of Cu bioavailability resulting from the oxidation of Cu(I) into soluble Cu(II). The high redox potential of the Cu(I)/Cu(II) couple confers cuproproteins the ability to directly oxidize substrates such as superoxides, ascorbates or phenolates. (Osman & Cavet 2008; Argüello et al. 2013).

Cu is essential to bacteria as it is an important redox factor for different enzymes as the cytochrome c oxidase or the superoxide dismutase (Bondarczuk & Piotrowska-Seget 2013; Ladomersky & Petris 2015). However, its high redox potential can be deleterious for the organism when its concentration increases. On the one hand, Cu can trigger a Fenton and Haber-Weiss reactions leading to an oxidative stress (Kimura & Nishioka 1997). On the other hand, Cu can also disrupt Fe-S clusters as it forms more stable interactions with S than Fe ions (Irving & Williams 1953; Ladomersky & Petris 2015).

Owing to Cu toxicity at high concentrations, bacteria have evolved multiple mechanisms to control Cu homeostasis and to prevent Cu-induced toxicity. First of all, Cu-containing proteins are not located in the cytoplasm but in the periplasm of Gram-negative bacteria, in cyanobacteria thylakoids or secreted by Gram-positive (Osman & Cavet 2008; Ladomersky & Petris 2015). Secondly, bacteria have evolved multiple detoxifying systems to cope with Cu stress. For example, *E. coli* has 2 chromosome-encoded mechanisms involved in Cu homeostasis, Cus and Cue systems, as well as a plasmid-borne system, Pco mechanism (Rensing & Grass 2003; Osman & Cavet 2008). The former is composed of seven genes, *pcoABCDRSE*. PcoA and PcoC are periplasmic proteins that detoxify Cu(I) into Cu(II). Also present in the periplasm, PcoE interact with Cu. The PcoB is thought to export Cu(II) outside of the periplasm. On the opposite, PcoD seems to transport Cu to the cytoplasm. PcoRS are two-component regulators that control other *pco* genes expression (Rensing & Grass 2003).

III. *Caulobacter crescentus*

It was previously shown in the laboratory that the oligotrophic and aquatic α -proteobacteria *C. crescentus* triggers a bimodal response to Cu stress relying on its intrinsic cell dimorphism (Lawarée et al. 2016). The *C. crescentus* asymmetric cell cycle yields a motile swarmer (SW) cell and a sessile stalked (ST) cell competent for DNA replication. In order to replicate its DNA and proceed to cell division, the SW cell must first differentiate into a ST cell (Ely 1991; Laub et al. 2007; Curtis & Brun 2010). Under Cu stress, the PcoA protein present in ST cells can detoxify Cu(I) and Cu(II). This ion is then expelled from the cytoplasm by PcoB. On the other side, the SW cell accumulates Cu within 1 min and immediately triggers a flight response to find a Cu-free environment where it will differentiate and proliferate (Lawarée et al. 2016). It was hypothesized that a chemotaxis pathway could, therefore, play a role in this response. In this respect, the *C. crescentus* will be discussed as well as the chemotaxis system present in these bacteria.

A. Cell cycle

C. crescentus has been extensively studied as a model for development as well as spatial and temporal gene expression control since this bacterium can undergo 2 different developmental processes (Fig. 8) (Curtis & Brun 2010). The first one concerns SW cells, this morphotype has a flagellum and multiple pili. After a period of motility is completed, it undergoes a SW-to-ST differentiation by losing its flagellum. Pili are disassembled and biogenesis of the stalk and the holdfast to the flagellum pole begin. Once the ST cell is differentiated, it can initiate the chromosome replication (Laub et al. 2007; Curtis & Brun 2010).

The developmental process associated with the ST cell is known to be cyclic as this morphotype returns to its predevelopmental stage. After DNA replication, the cell begins to grow and ultimately form a predivisional (PD) cell. Cytoplasmic compartmentalization leads to divergent genetic programs in each cell. For example, the future SW daughter cell sees its flagellum synthesized at the pole opposite to the stalked pole (Skerker & Laub 2004; Schrader et al. 2016). After the chromosome segregation and division, the 2 daughter cells are totally functional: ST cell can undergo another division while SW cell can swim away and differentiates into another ST cell (Laub et al. 2007; Curtis & Brun 2010).

B. Chemotaxis system

The SW cell is mobile and movements are biased by a chemotaxis system. The predicted chemotaxis protein-encoding genes are organized into 2 operons, with additional *mcp* and *che* genes dispersed across the genome. In total, there are 19 predicted *mcp* genes and 2 *cheA* genes. Redundancy also concerns *cheY*, *cheB* and *cheR* genes. In addition, predicted chemotaxis proteins such as CheU and CheE seem to be specific to *C. crescentus* (Nierman et al. 2001).

In the PD cell, chemotaxis proteins are transcribed and the chemosensory array is incorporated into the flagellated pole during this stage. This incorporation seem to specifically happen in the vicinity of the flagella of the SW cell (Gomes & Shapiro 1984; Nathan et al. 1986; Briegel et al. 2008). The targeting of the MCP to the SW inner membrane is thought to occur through its N-terminal end (Alley et al. 1992). It has been shown that the polarity determinant TipN/F plays a role in the identification of the flagellated pole, in the placement of the flagellum and the chemosensory cluster (Huitema et al. 2006).

In the genome of *C. crescentus*, there are 12 annotated *cheY* genes but no known phosphatase gene (Nierman et al. 2001). It has been observed that at least 2 CheY proteins can interact with FliM, leading to complex responses (Morse et al. 2015). Due to the important number of *cheY* genes, the absence of any phosphatase could be compensated by a phosphate sink as observed in *R. sphaeroides* (Porter et al. 2008; Morse et al. 2015). Nonetheless, a novel family of CheY-like (Cle) proteins has been recently identified in *C. crescentus*. These proteins seem to be activated by cyclic-di-GMP through an additional domain in the C-terminus. Like their orthologues, Cle proteins are able to interact with FliM, a protein of the flagellar motor to adjust speed or switching frequency (Nesper et al. 2017). These proteins could also have a role in surface recognition, in differentiation from SW to ST with holdfast synthesis and in the attachment to the surface (Hughes & Berg 2017; Nesper et al. 2017).

Objectives

As described previously, the redundancy of Che proteins lead notably to complex signalling pathway, resulting in adapted responses of the bacteria to environmental fluctuations. Moreover it has been previously shown that *C. crescentus* SW cells can flee Cu and it is thought that this flight is mediated by chemotaxis. The actors involved in Cu-induced negative chemotaxis are not known.

In this purpose, the first objective of this master thesis was to understand the role of *C. crescentus* CheAI and CheAII in Cu negative chemotaxis. First, a bioinformatics analysis was performed to predict the protein structure and the possible contribution of each protein in chemotaxis; CheAI and CheAII were compared to CheA from model organisms such as *E. coli* and *Thermogota maritima*. Then, the presence and the possible common origin of *cheAI* and *cheAII* operons was assessed in Proteobacteria containing at least 2 *cheA* genes *via* synteny analysis. Knock-out strains for *cheAI/II* genes were constructed and the growth and the chemotaxis ability were characterized for each strain. As described in the literature, *che* genes are expressed in the PD cell. However, no precise data is available for *cheAI/II* genes in normal conditions. To assess the expression of these genes, RT-qPCR was performed.

The second aspect of this study will be devoted to the identification of other proteins involved in Cu-induced chemotaxis actors by genetic screen. With this respect, a chemotaxis assay was developed and transpositional mutants with impaired Cu flight responses were isolated and characterized.

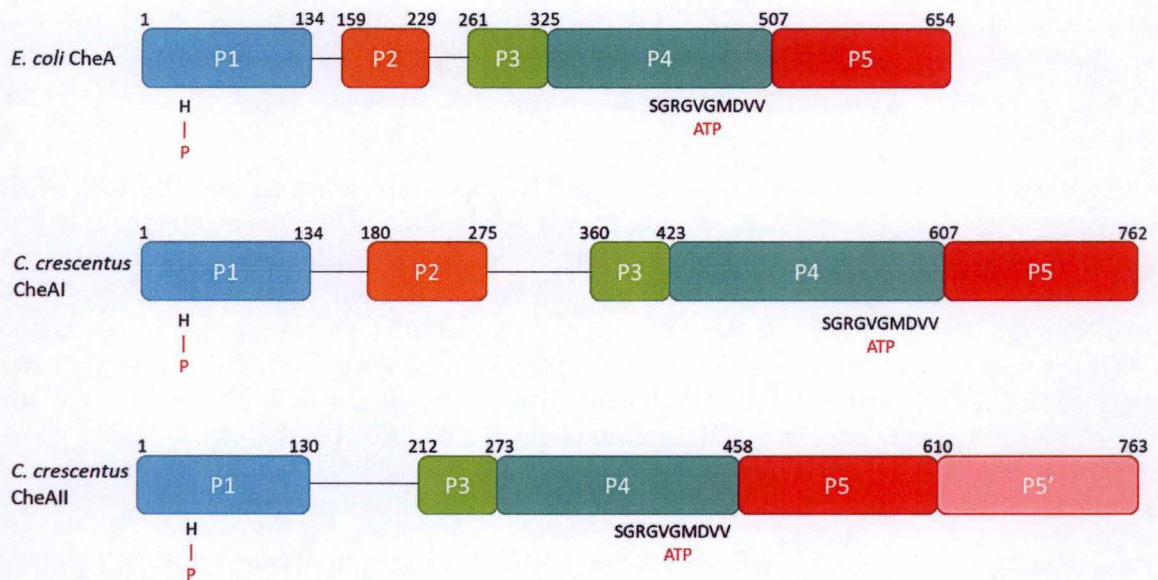


Figure 9. *Caulobacter crescentus* CheAI/II protein structure predictions. The position of each domain of *C. crescentus* CheAI and CheAII proteins was first assessed using homologies with *E. coli* CheA. In addition, secondary structure prediction performed by JPred4 confirmed previous observations. In both CheAI and CheAII important residues are conserved such as the phosphorylated histidine or the ATP binding pocket. Nonetheless, CheAII protein is missing a P2 domain but has a second P5 domain (Notredame et al. 2000; Mo et al. 2012; Drozdetskiy et al. 2015).

Results and discussion

I. *In silico* characterization of *cheA* genes and protein

A. CheAI structure is typical while CheAII protein seems to be unique

To gain some insights on the predicted structure and function of *C. crescentus* CheAI and CheAII proteins, different approaches were used. The first one was to identify domains by multiple sequence alignment using T-Coffee with *C. crescentus* CheAI, CheAII, *E. coli* CheA and a well-studied homolog, CheA from *Thermogota maritima* (Notredame et al. 2000). Since the position of each domain has been determined in *E. coli* CheA, homologies were used to position CheAI and CheAII domains (Fig. S1, Fig. S2) (Mo et al. 2012). In addition, secondary structure prediction was performed for each protein using JPred4 to confirm each domain position and identity (Drozdetskiy et al. 2015; Webb & Sali 2016).

As described previously, CheA protein is composed of 5 distinct domains. The P1 domain contains a histidine which is phosphorylated by the P4 domain. The P3 domain is responsible for dimerization while P2 and P5 domains interact with RR, and MCP and CheW, respectively. With the exception of the P2 domain, all domains are conserved among *E. coli*, *T. maritima* and *C. crescentus* CheA proteins. In addition, some amino acids are highly conserved in both CheAI and CheAII, such as the phosphorylated histidine in P1 domain and the ATP-binding pocket in P4 domain (Fig. 9) (Bilwes et al. 1999; Nishiyama et al. 2014; Briegel et al. 2012).

Interestingly, CheAI P2 domain shows a higher divergence and does not appear to be tightly conserved among CheA proteins. Nevertheless, the secondary structure of this domain displays a predicted pattern of α helices and β sheets homologous to solved P2 structures (Fig. S1) (Mo et al. 2012). The differences present in this domain could underlie the coevolution between the histidine kinase and its response regulators (RR) to maintain a proper interaction and therefore, the chemotaxis ability (Mo et al. 2012). On the other side, it has been shown in *E. coli* that CheA directly interacts with non-chemotaxis proteins such as EI (enzyme I) from the PTS pathway (Wadhams & Armitage 2004). This interaction suggests the adaptation of the CheA protein to this unusual binding implies a specific structure that would allow binding with different proteins.

On the contrary, multiple sequence alignment and secondary structure prediction did not highlight the presence of any P2 domain for CheAII (Fig. 9). The amino acid sequence between P1 and P3 domains was smaller than expected and does not seem to have a particular structure, suggesting the absence of a response regulator binding domain. As the P2 domain docks CheY and increases phosphorylation rates by P1, it suggests that CheAII participation in response regulator phosphorylation would not be as important as CheAI. Nevertheless, it has been proven that sole P1 domain can phosphorylate CheY *in vitro* and does not require any P2 domain (Mo et al. 2012; Mourey et al. 2001). In *R. sphaeroides*, the heterodimer CheA₃CheA₄ is functional and does not contain any P2 domain. This heterodimer is specific to cytoplasmic MCPs and responsible for their signal transduction (Porter & Armitage 2004). Since some *C. crescentus* MCPs are predicted to be cytoplasmic, one could imagine that CheAII is specifically localized in this chemoreceptor array.

As observed in available CheA structure models, the P3 domain from both CheAI and CheAII proteins was predicted to be composed of 2 α helices (Fig. S1, Fig. S2). The dimerization of 2 P3 domains is based on the hydrophobic interactions of these 2 secondary structures (Bilwes et al. 1999). Moreover, the α helices would be located in the same region than in the *E. coli* and *T. maritima* CheA homologous P3 domains, reinforcing the hypothesis that CheAI and CheAII

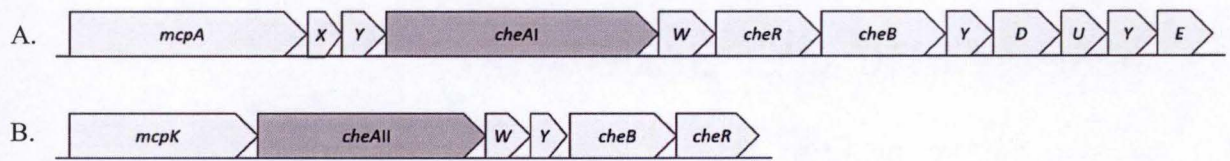


Figure 10. Organization of *che* operons in *C. crescentus*. **A.** First chemotaxis operon found in the genome, which contains *cheAI* gene (CCNA_00442) and referred to as *cheAI* operon. **B.** Second chemotaxis operon with *cheAII* gene (CCNA_00630) and cited as *cheAII* operon. Representation is relative to real gene length (Nierman et al. 2001; Caspi et al. 2016).

form functional dimers. These dimers could be homodimers or heterodimers, with one CheAI subunit and one CheAII subunit, such as CheA₃ and CheA₄ in *R. sphaeroides* (Porter & Armitage 2004).

The *C. crescentus* CheAII protein seemed to have a second P5 domain in its C-terminal end (Fig. 9). This additional domain displayed homologies with CheA P5 domain with a similar pattern of α helices and β sheets found (Fig. S2). The presence of a potential second P5 domain has never been described so far. CheW-CheA interaction is necessary to anchor CheA to MCPs and CheW is also required for assembly of MCPs clusters coupled with CheA proteins (Jones & Armitage 2015). With this respect, CheAII protein could potentiate chemoreceptor arrays scaffolding, where the second P5 domain would substitute CheW. This scaffolding role could be completed by the formation of CheAII homodimers or CheAI/II heterodimers. The potential scaffolding role of CheAII could solely keep MCP proteins together while heterodimers could help anchoring CheAI protein to MCPs. Therefore, it increases the signal sensitivity and the response efficiency. The presence of heterodimers has already been described in *R. sphaeroides* (Porter & Armitage 2004).

B. *cheAI* operon seems to be more conserved than *cheAII* operon

The chemotaxis protein redundancy in *C. crescentus* does not concern only the CheA protein but also other chemotaxis proteins such as CheY, CheB and CheR. The genes coding for these proteins are organised in 2 chemotaxis operons with different organizations (Fig. 10) (Nierman et al. 2001). To determine whether this chemotaxis cluster redundancy is restricted to *C. crescentus*, several proteobacterial genomes were selected based on previous phylogenetic analyses and the number of *cheA* genes was determined (Williams et al. 2010; Williams et al. 2007; Gupta 2006; Gupta 2000; Caspi et al. 2016). The number of *cheA* genes in each genome was estimated based on genome annotation, and not based on sequence homologies since all CheA proteins are not similar (Caspi et al. 2016). Unfortunately, most organisms' genome annotation is only based on homology and therefore, some *cheA* genes could be missed due to a lack of annotation. When no annotated *cheA* could be found, a blast of *C. crescentus* CheAI protein against the considered genome was performed.

Out of the 129 examined Proteobacteria, 23 exhibited at least 2 *cheA* genes (Table S1). Some bacterial genomes harbour more than 2 homologous *cheA* genes such as *R. sphaeroides* and *M. xanthus*, which both possess 4 *cheA* genes. Interestingly, most of the organisms containing 2 chemotaxis operons are found either in aquatic or in soil environments, which are considered as complex environments. It has been shown that the number of chemotaxis systems could be linked to the bacteria lifestyle, with a higher number of *che* genes in complex ecological niches (Wuichet & Zhulin 2010). The redundancy of chemotaxis protein could help the bacteria to decipher complex signals in order to provide an adapted response, such as the *R. sphaeroides* chemotaxis system (Porter et al. 2008).

In order to determine whether chemotaxis operons are conserved and have potentially a common origin, bacterial species with 2 or more *cheA* genes were subjected to a synteny search (i.e. gene clusters with a locally conserved chromosomal organization) with the *C. crescentus* CB15N as the reference genome (Vallenet et al. 2009). Interestingly, the overall organization of the *cheAI* operon is conserved in most organisms, from *cheY* (CCNA_00441) to *cheYII* (CCNA_00446) genes (Table S2). *mcp* genes are usually poorly conserved and highly subjected to variations due to their ligand-specific binding and the diversity of ligands. The conservation pattern of the *cheAII* operon appears to be not as important as for the *cheAI* operon.

Only 5 out of the 23 organisms, all belonging to the α -proteobacteria class, showed a similar operon organization; *cheAII* operon homologous genes seemed to have another organization in

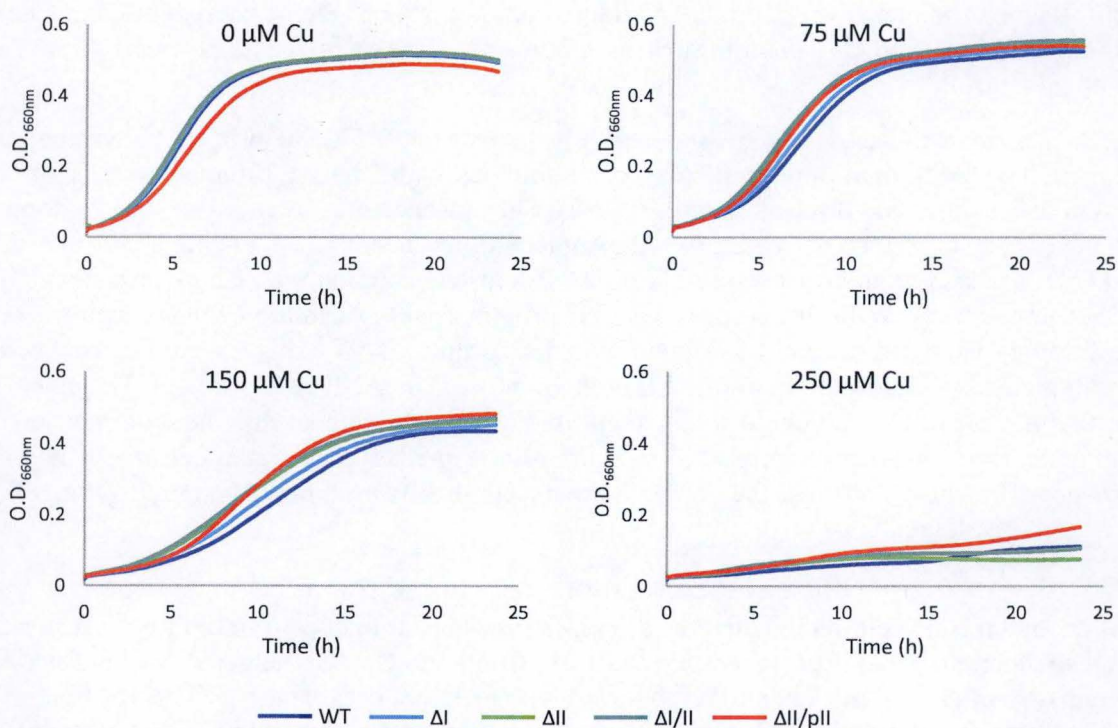


Figure 11. Growth profiles of *cheAI/I* knock out strains in absence or in presence of different Cu concentrations in PYE rich medium.

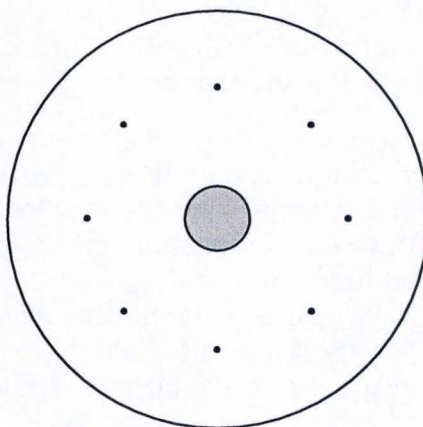


Figure 12. Chemotaxis assay plate design. The central plug is made of PYE 1.5 % agar and contains 5 mM of Cu. The motility medium, PYE 0.25 % agar, surrounds the plug. Colonies were insemminated at a fixed distance of the plug.

other Proteobacteria classes (Table S3). In other bacteria, *cheAII* operon genes homologues display another chemotaxis gene organization. This observation suggests that *cheAII* operon could be specific to α -proteobacteria and, at least, to some specific species. The environmental niche of the former organisms seems to embrace some complexity such as sediments, mud or sewage. Moreover, 4 bacteria can be found in association with other complex organisms such as *Methylobacterium nodulans*, a legume root-nodule-forming bacterium; *Pseudovibrio hongkongensis* in association with a marine flatworm (Polyclad) (Jourand et al. 2004; Xu et al. 2015). Chemotaxis could be important for these organisms in order to find and to enter in association with other organisms.

One of the lingering questions is about the role of the *cheAII* operon. In some organisms, chemotaxis proteins are not only involved in chemotaxis pathways but also in other processes such as biofilm formation, pili synthesis or pili-induced motility. For instance, *M. xanthus* chemotaxis operons have varied function other than chemotaxis (Zusman et al. 2007). This example suggests that *cheAII* operon could be involved in other pathways than chemotaxis.

II. Characterization of single and double *cheA* KO mutants

A. *cheA* KO mutant growth is not affected by Cu

Since CheA proteins have a role in development in some organisms (Zusman et al. 2007), the deletion of *C. crescentus cheA*/II genes could have an effect on growth. Moreover, the proteins resulting from these genes could have an effect on Cu-induced negative chemotaxis and therefore, on growth in presence of Cu. In this respect, we monitored the growth of $\Delta cheA$, $\Delta cheAII$, $\Delta cheA$ /II and $\Delta cheAII$ /*pcheAII* mutants in presence of increasing Cu concentrations (Fig. 11). It appeared that all of these strains grew in a similar way to the WT strain in presence of Cu. We could conclude that the deletion of *cheA*/II genes in *C. crescentus* has no impact on growth and therefore, proteins were involved in growth independent pathways.

B. CheA seems to be the main chemotaxis histidine kinase involved in Cu-induced chemotaxis

In *E. coli*, the deletion of *cheA* gene led to a non-chemotactic mutant since the CheA protein has a central role in chemotaxis (Wadhams & Armitage 2004). In order to assess and to quantify the chemotactic capacities of the *C. crescentus cheA* mutants, a chemotaxis assay was developed during this master thesis. The design is the following: (1) a 1.5 % agar plug containing 0, 3 or 5 mM Cu was placed at the centre of a dish and (2) soft-agar 0.25 % agar medium was poured into the space surrounding this plug (Fig. 12). Following a 48 h incubation, the Cu-induced negative chemotaxis is quantified by calculating a ratio between the inner and outer radius of the colony, using ImageJ (Fig. 13) (Schneider et al. 2012). This ratio is used to evaluate the negative chemotaxis since the Cu-containing plug was expected to trigger bacterial flight (in the inner radius), generating asymmetrical swarming colonies (Fig. 13A and 13B). The comparison of 0 mM and 5 mM in plug-Cu conditions ratio suggests a negative chemotaxis induced by Cu, considering the ratio significant difference (Fig. 13C) ($p < 0.001$, $N = 16$, using ANOVA). In the case of a chemotaxis defect, the mutants should show a different phenotype compared to the WT such as a smaller colony or a higher inner/outer radius ratio, suggesting a Cu flight decrease.

The $\Delta cheA$ and the $\Delta cheA$ /II mutants did not seem chemotactic as they could not form a motility halo on swarmer plates (Fig. 14A and 14B). These observations were not due to a motility defect since both strains were motile and the SW cells had a normal run-reverse-flick swimming pattern (Table 1). The absence of CheA likely prevent CheY phosphorylation and therefore, the bacteria movements are not biased. However, this hypothesis does not fully

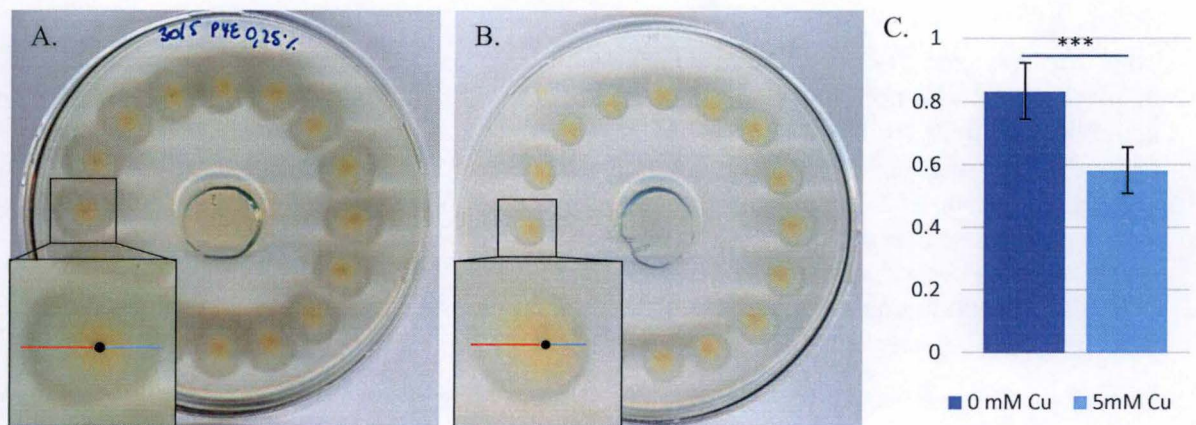


Figure 13. Quantification of Cu-induced chemotaxis in *C. crescentus* WT strain. A. Chemotaxis assay with PYE 1.5 % agar plug containing no Cu (A.) or 5 mM Cu (B.). C. Inner (in blue)/outer (in orange) radius ratio of *C. crescentus* WT colonies in chemotaxis assay in absence or in presence of copper. The ratio is used as an indication for copper-induced negative chemotaxis. Compared to the negative control where no Cu is present, the inner radius decreased which suggests a copper flight. Error bars represent \pm standard deviation. ***, $p \leq 0.001$ using ANOVA, $N = 16$.

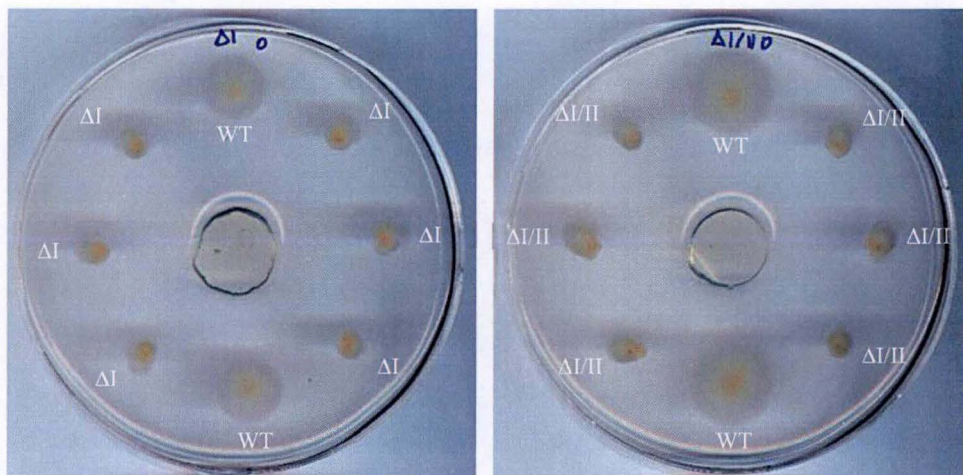


Figure 14. Chemotaxis ability of $\Delta cheAI$ and $\Delta cheAI/II$ on swarmer plates in absence of Cu.

Table 1. Motility, swimming and chemotaxis characteristics from $\Delta cheA$ strains.

Strains	Motility	Swimming pattern conservation	Chemotaxis
$\Delta cheAI$	+	+	-
$\Delta cheAII$	+	+	+
$\Delta cheAIV/II$	+	+	-

explain why bacteria do not disperse on the plate. A second aspect of the swimming pattern has to be taken in account which is the forward run angle. The swimming of unflagellated bacteria is not straight and it eventually results in circular trajectories (Morse et al. 2015). In absence of biased movements, *C. crescentus* $\Delta cheAI$ and the $\Delta cheAI/II$ strains end swimming in circles.

Concerning $\Delta cheAII$ mutant, the observed phenotype on swarmer plates in presence of Cu was comparable to the WT phenotype (Fig. 15A). Due to technical issues, the chemotaxis assay of $\Delta cheAII$ could not be performed in absence of Cu. By measuring the inner and the outer ratio of each colony, the inner/outer ratio was calculated and the negative chemotaxis to Cu was quantified. It appeared that ΔII had a similar behaviour to the WT strain upon Cu stress (Fig. 15B).

However, the overexpression of *cheAI* in the strain $\Delta cheAII/pcheAII$ did not impair Cu-induced chemotaxis (Fig. 16A and 16B) but the colony size was smaller, compared to WT and $\Delta cheAII$ strains (Fig. 16A and 16C). Each colony area was measured using ImageJ (Schneider et al. 2012) and statistical analyses revealed a significant decrease of chemotaxis halo ($p < 0.001$, $N_{WT} = 4$; $N_{\Delta cheAII} = 6$; $N_{\Delta cheAII/pcheAII} = 6$; using T-test). This smaller colony size could be due to impaired chemotaxis, caused by overexpression of *cheAII* since it could replace CheAI proteins in chemotaxis clusters. As predicted by bioinformatics, the protein structure of CheAII is unusual and 2 of its features could decrease chemotaxis pathway efficiency. First, the absence of any P2 domain could decrease the phosphorylation rate of RRs as these are not docked anymore. Secondly, the 2 P5 domains could replace CheW and/or CheAI in chemotaxis array, disturbing them and, eventually, impair signal transduction.

To confirm those results, a live chemotaxis imaging assay was used (Lawařée et al. 2016). This assay is based on a PDMS chamber mounted on a glass slide where a Cu-containing and a control agarose plugs were casted before injecting SW cells (Fig. 17A). After injection, the SW cells population was monitored for 25 min by time-lapse microscopy in the vicinity of each plug. The chemotaxis ability of each strain was quantified by measuring the SW cell population dynamics (Fig. 17B). Consistent with the chemotaxis assay, WT cells exhibited a negative chemotaxis to Cu since the number of SW decreases by around 50 % after 25 min (Fig. 18A). As expected, the same behaviour was observed for the $\Delta cheAII$ mutant (Fig. 18C). However, no population decrease was observed in the vicinity of the Cu plug for $\Delta cheAI$ and $\Delta cheAI/II$ mutants (Fig. 18A and 18B).

All of these chemotaxis data suggests that CheAI is the main histidine kinase involved in chemotaxis and more precisely, in Cu-induced chemotaxis. In absence of any functional *cheAI* gene, the whole chemotaxis is impaired and CheAII does not seem to be able to compensate CheAI absence. Another observation reinforcing this hypothesis is the absence of any difference in chemotaxis phenotype between $\Delta cheAI$ and $\Delta cheAI/cheAII$ mutants. On the other side, the deletion of *cheAII* does not seem to impair *C. crescentus* chemotaxis ability since the observed phenotype is similar to the WT strain. Nevertheless, overexpression of CheAII negatively impacted chemotaxis, suggesting that CheAII could be able to interact with chemotaxis clusters.

III. Expression of *cheA* genes

It has been previously shown that chemotaxis clusters are mainly synthesized in the PD cell so the SW is directly competent for taxis (Curtis & Brun 2010). To determine whether *cheAI* and *cheAII* exhibit the same pattern of expression, we measured the expression of these 2 genes by RT-qPCR in the SW, ST and PD cells under basal conditions.



Figure 15. Cu-induced chemotaxis in $\Delta cheAII$. **A.** The Cu chemotaxis phenotype of $\Delta cheAII$ is similar to the WT strain in presence of increasing Cu concentration. **B.** Quantification of the Cu negative chemotaxis by measuring inner/outer radius ratio. Mean \pm standard deviation. No significant difference using T-test.

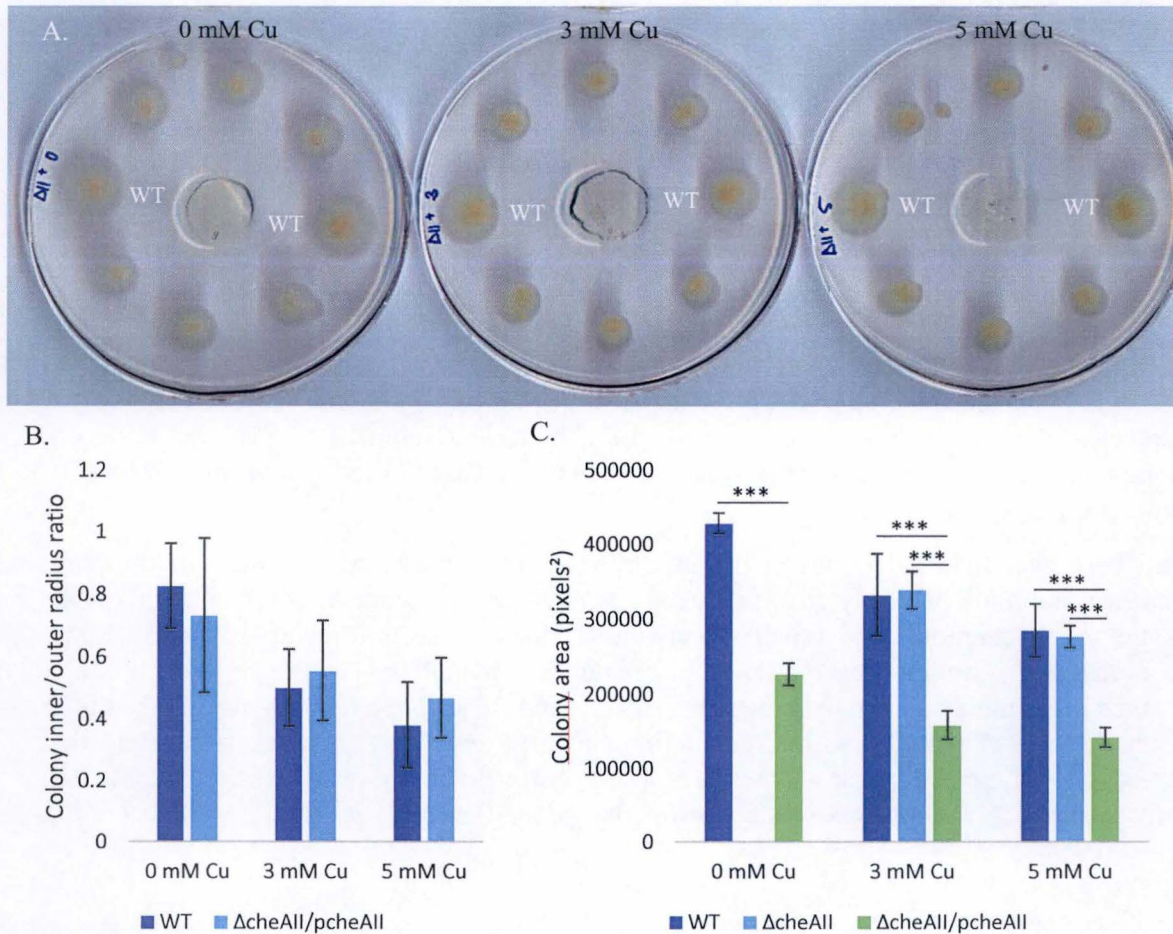
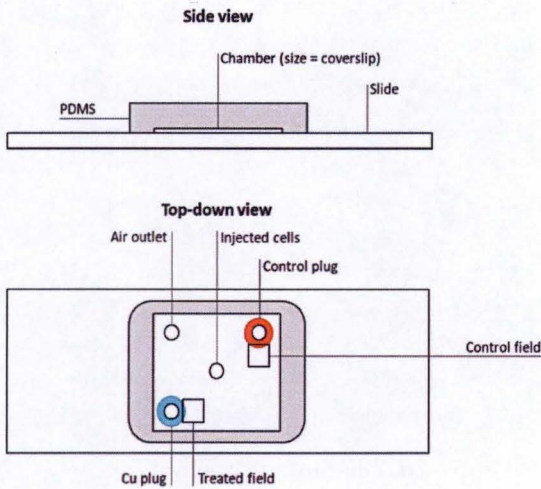


Figure 16. Chemotaxis phenotype of $\Delta cheAII/pcheAII$ in absence and in presence of Cu. **A.** Cu chemotaxis phenotype of $\Delta cheAII/pcheAII$. **B.** The Cu-induced negative chemotaxis was not impaired upon overexpression of *cheAI* by measuring the inner/outer radius ratio. **C.** The colony size measured by ImageJ (Schneider et al. 2012) of $\Delta cheAII/pcheAII$ was significantly smaller than the halo formed by WT and $\Delta cheAII$ strains in absence or presence of different Cu concentrations. Mean \pm standard deviation. ***, $p \leq 0.001$ using T-test; $N_{WT} = 4$; $N_{\Delta cheAII} = 6$; $N_{\Delta cheAII/pcheAII} = 6$.

A.



B.

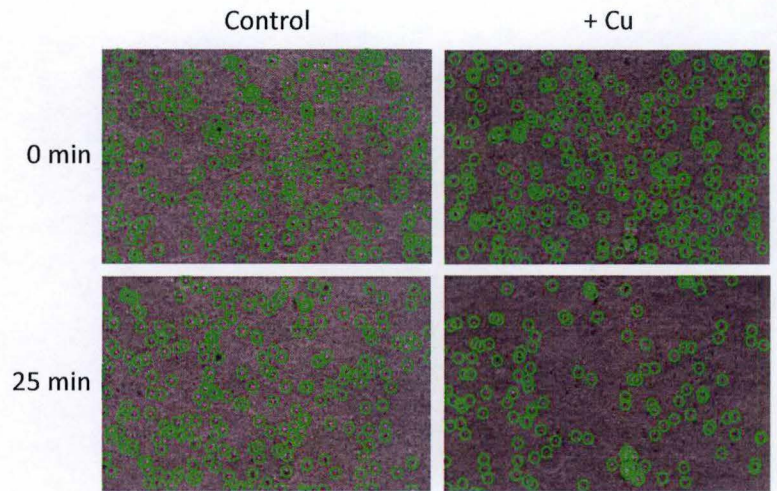


Figure 17. Live chemotaxis assay. **A.** Schematic representation of the Live Imaging Assay device (side and top-down views). **B.** Matlab detection of SW cells located in the vicinity of the control or Cu plugs at times 0 and 25 min post inoculation.

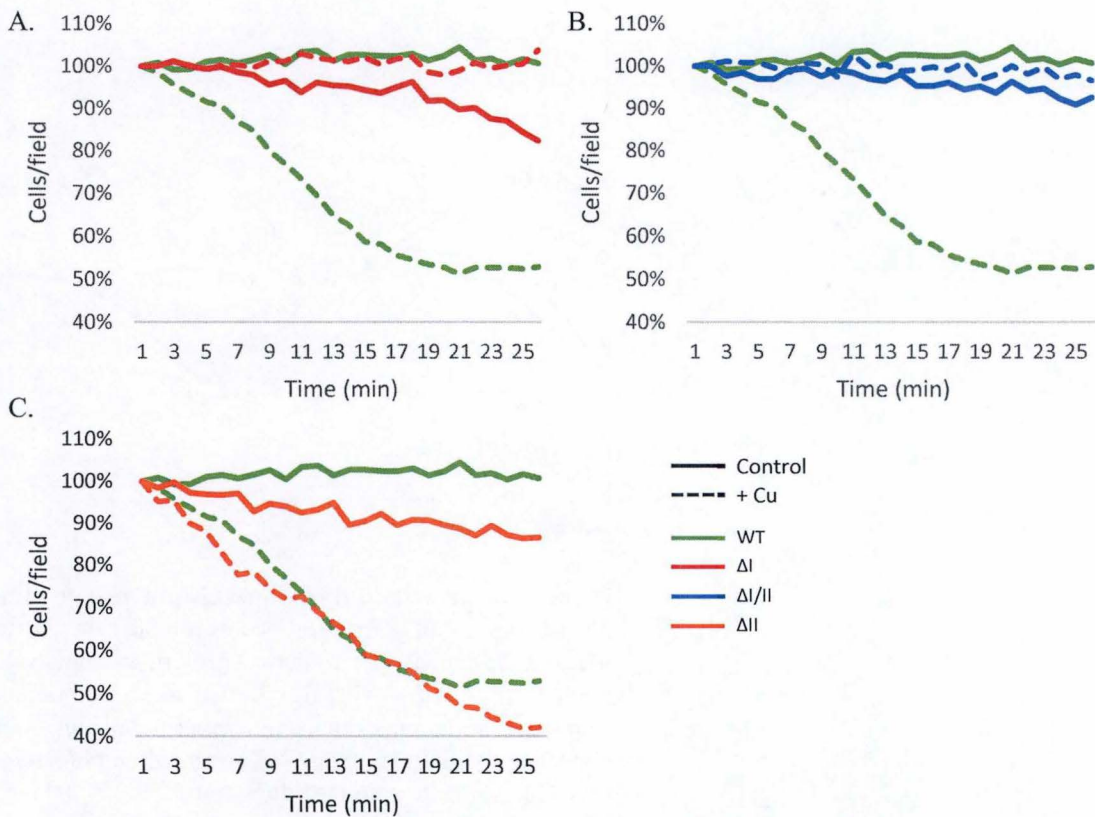


Figure 18. Cu-induced flight response in SW cells of *cheA* knock out backgrounds. Trend curves represent the percentage of WT (green), $\Delta cheA I$ (red), $\Delta cheA I/II$ (blue) or $\Delta cheA II$ (orange) SW cells in the vicinity of the control plug (continuous line) or the Cu plug (dotted line). **A.** Up to 50% of WT SW cells flee copper stress, $\Delta cheA I$ SW cell percentage is constant, meaning that this strain does not flee Cu. **B.** $\Delta cheA I/II$ SW cell percentage is constant, meaning that this strain does not flee Cu. **C.** The $\Delta cheA II$ strain seems to respond negatively to Cu plug and the flight response is similar to WT strain.

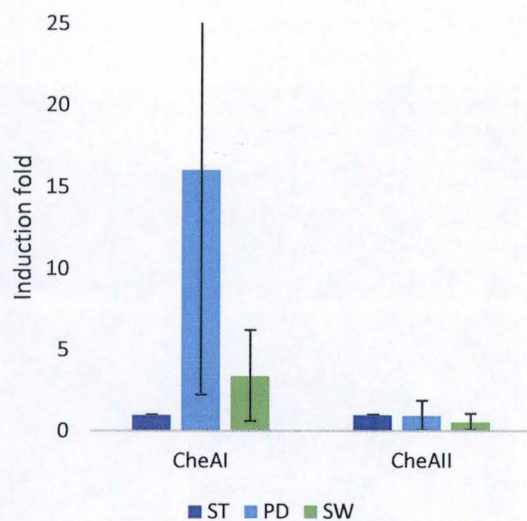


Figure 19. *cheAI/II* mRNA levels in ST, PD and SW cells. Mean \pm standard deviation; biological replicates = 4; technical replicates = 4.

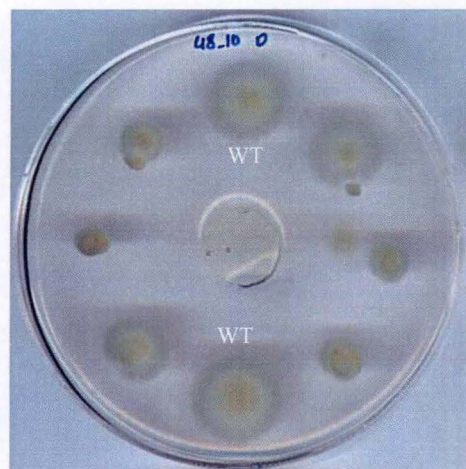


Figure 20. Chemotaxis phenotype of mutant 48_10 on swarmer plates in absence of Cu.

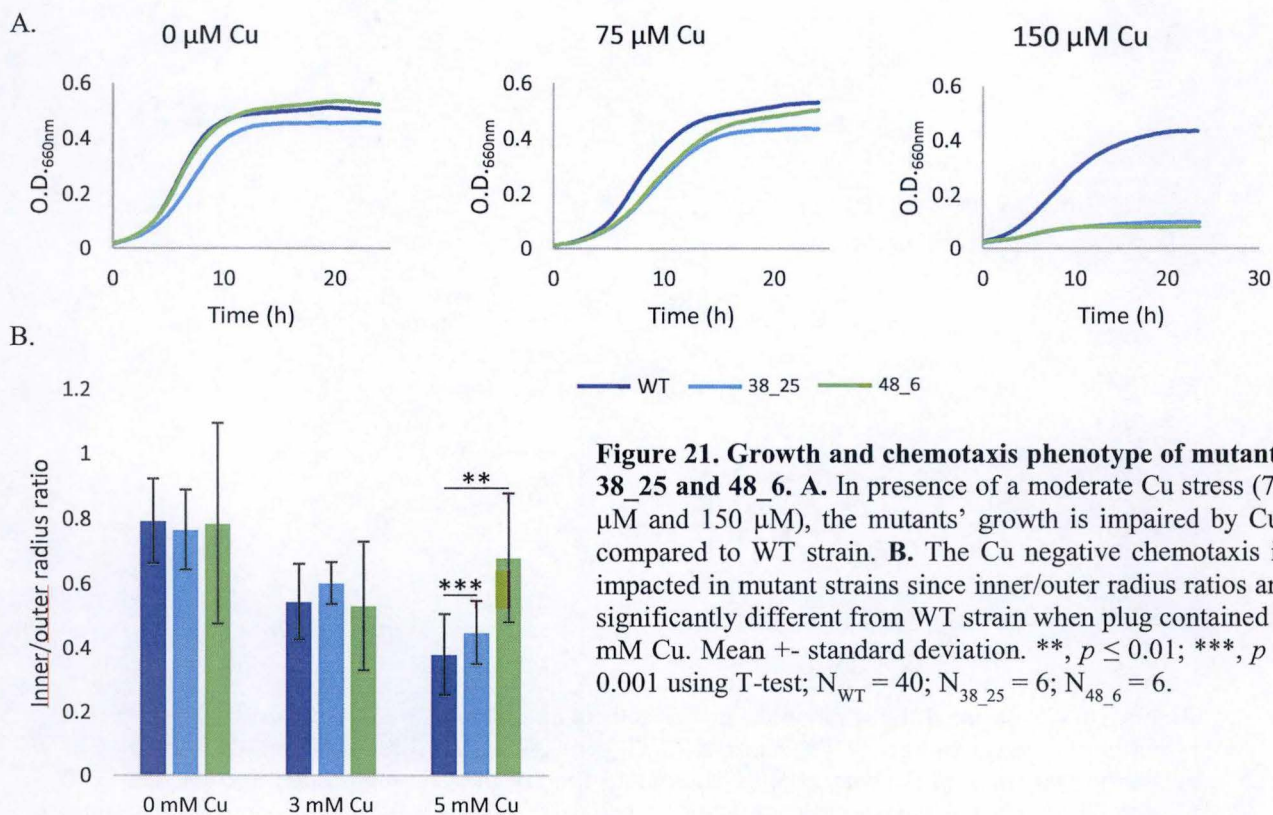


Figure 21. Growth and chemotaxis phenotype of mutants 38_25 and 48_6. **A.** In presence of a moderate Cu stress (75 μM and 150 μM), the mutants' growth is impaired by Cu, compared to WT strain. **B.** The Cu negative chemotaxis is impacted in mutant strains since inner/outer radius ratios are significantly different from WT strain when plug contained 5 mM Cu. Mean \pm standard deviation. **, $p \leq 0.01$; ***, $p \leq 0.001$ using T-test; $N_{\text{WT}} = 40$; $N_{38_25} = 6$; $N_{48_6} = 6$.

cheAI expression mainly occurred in PD cells and the lowest expression induction was observed in ST cells (Fig. 19). These observations are consistent with what have been described previously. Moreover, it supports the idea that CheAI has a potential role in chemotaxis. Surprisingly, the expression of *cheAII* appeared to occur in PD cells as well as in ST cells (Fig. 19). The expression of a chemotaxis protein in the ST cell has never been reported previously in *C. crescentus*. In agreement with the atypical structure of CheAII, this protein could be implicated in another pathway than chemotaxis which could take place in the ST cells. This could correspond with what is observed in *M. xanthus* (Zusman et al. 2007). Nonetheless, $\Delta cheAII$ and $\Delta cheAI/II$ did not show any developmental defect and the global phenotype of both strains is comparable to the WT strain under the tested conditions. To further investigate this hypothesis, further bioinformatics analyses could be performed in order to eventually find potential interactant of CheAII and to compare the CheAII operon development-related operons.

IV. Isolation and characterization of chemotaxis mutants

In order to find other actors involved in the Cu-induced chemotaxis, a transpositional mutant library was created and screened. Mini-Tn5 transposons were inserted in the WT strain; where transposition event should occur statistically every 200 bp, potentially disrupting every gene. This can be explained by the mean gene size in *C. crescentus* which is 969 bp and that there are no non-coding regions in bacteria (Nierman et al. 2001). Transposition was chosen since transposon insertion site is easily identifiable by a semi-arbitrary PCR (see Experimental Procedures for further details) and by comparison with the genome sequence. In this purpose, a large-scale Cu chemotaxis assay has been developed during this master thesis, of which the design has been described previously.

Out of more than 5000 screened mini-Tn5 mutants, 23 candidates were isolated. The selection of candidates was based on the chemotaxis phenotype to Cu (decreased flight) or on the size of the chemotactic halo (smaller compared to the WT strain). After growing on chemotaxis plates in presence of a 5 mM Cu-containing plug, clones were tested in absence and in presence of increasing Cu concentrations (0 mM, 3mM and 5 mM). This second screening allowed us to select the mutants defective for chemotaxis in the presence of Cu only. Unfortunately, we never observed a complete chemotaxis defect, but rather a reduced flight from Cu, characterized by a higher inner/outer radius ratio relative to the WT strain. However, the most represented mutant phenotype consisted in a reduced size of the colony in the presence of Cu, suggesting an increased Cu sensitivity.

The 23 isolated mutants were further characterized in term of growth, motility (visual observation under the microscope) and chemotaxis. Only one mutant (48_10) was not motile, which resulted in the absence of a motility halo on plate. (Fig. 20). The gene disrupted by the transposon is involved in pseudaminic acid synthesis (CCNA_02961). It has been shown in *Campylobacter jejuni* that this 2-keto-3-deoxy acid is responsible for flagellum glycosylation which is essential for flagella development and for motility (Chou et al. 2005). The motility defect of the 48_10 mutant suggests that a similar flagellum glycosylation occurs in *C. crescentus* and that this modification should be important for motility. Nonetheless, the 48_10 mutant did not shown Cu sensitivity when assessed for growth.

38_25 and 48_6 mutants' growth was slightly impaired in the presence of Cu (Fig. 21A). Moreover, the chemotaxis phenotype of the candidates showed a significant decrease of Cu-induced flight (**, $p \leq 0.01$; ***, $p \leq 0.001$ using T-test; $N_{WT} = 40$; $N_{38_25} = 6$; $N_{48_6} = 6$) (Fig.

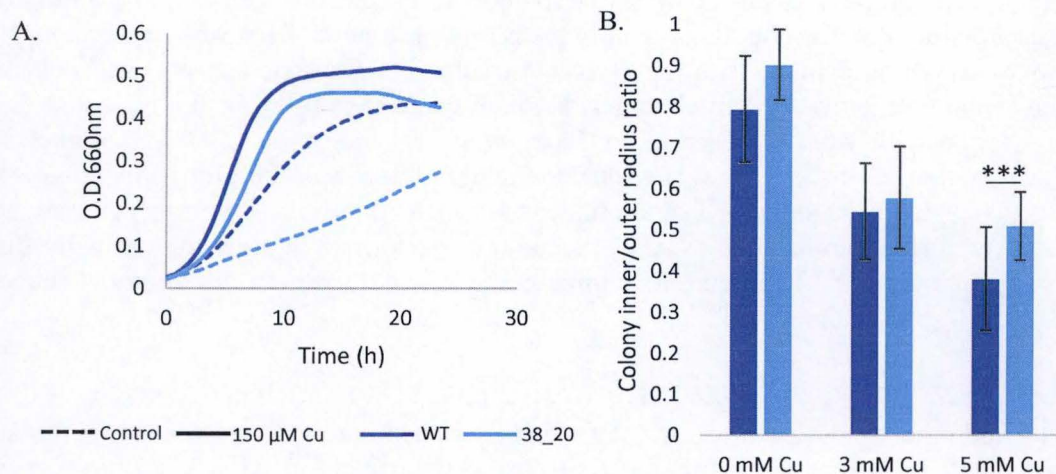


Figure 22. Growth and chemotaxis phenotype of mutant 38_8. **A.** In presence of a moderate Cu stress (dotted line), the mutant's growth is impaired by Cu, compared to WT strain. **B.** The Cu negative chemotaxis is impacted in mutant strain since inner/outer radius ratios is significantly different from WT strain when plug contained 5 mM Cu. Mean \pm standard deviation. ***, $p \leq 0.001$ using T-test; $N_{WT} = 40$; $N_{38_20} = 6$.

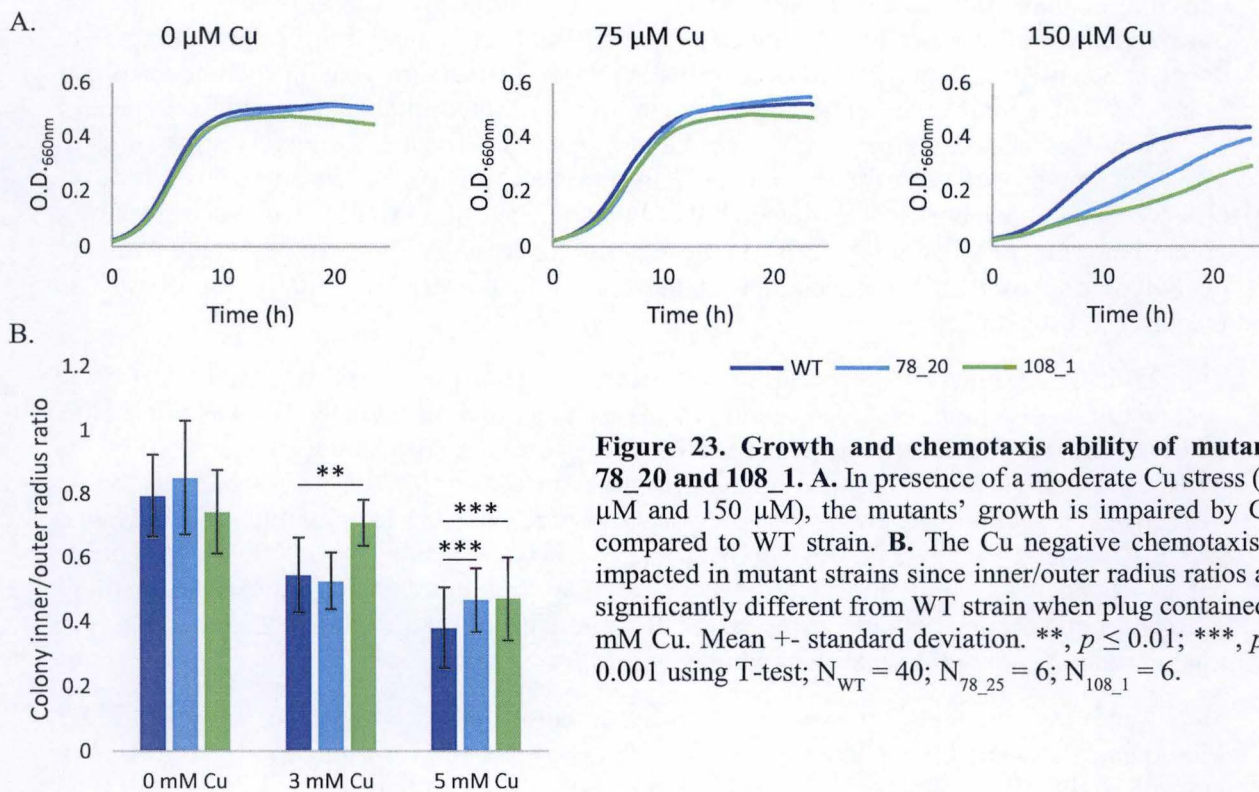


Figure 23. Growth and chemotaxis ability of mutants 78_20 and 108_1. **A.** In presence of a moderate Cu stress (75 μM and 150 μM), the mutants' growth is impaired by Cu, compared to WT strain. **B.** The Cu negative chemotaxis is impacted in mutant strains since inner/outer radius ratios are significantly different from WT strain when plug contained 5 mM Cu. Mean \pm standard deviation. **, $p \leq 0.01$; ***, $p \leq 0.001$ using T-test; $N_{WT} = 40$; $N_{78_25} = 6$; $N_{108_1} = 6$.

21B). The transposon disrupted the same gene, meaning that the 2 isolated strains could derive from the same mutant. The involved gene is a transcriptional regulator (CCNA_00852), part of the TetR/AcrR family. This family is part of the one-component systems which are usually involved in antibiotic resistance and regulation of genes encoding small-molecules exporters. TetR family regulator ComR from *E. coli* controls the expression of ComC, a protein involved in outer membrane permeability to Cu (Cuthbertson & Nodwell 2013). Unfortunately, the alignment of *E. coli* ComC and CCNA_00852 did not highlighted homologies between the 2 proteins as they only share 23 % identity (Camacho et al. 2009). The absence of homology does not mean that the function is not similar and the proteins could have evolved independently and led to the same function. To confirm that CCNA_00852 is implicated in the Cu permeability, the accumulation of Cu could be monitored in strains 38_25 and 48_6. The intracellular Cu concentration can be measured by atomic absorption spectroscopy as previously performed for the WT strain (Lawarée et al. 2016). In the case of an increased Cu permeability, one could expect higher cytoplasmic and periplasmic Cu concentration (Mermod et al. 2012).

The candidate 38_8 growth and chemotaxis ability were also impacted in presence of Cu stress (***, $p \leq 0.001$ using T-test; $N_{WT} = 40$; $N_{38_20} = 6$) (Fig. 22A and 22B). In this mutant, the mini-Tn5 inserted inside the CCNA_03496 gene which encodes the cytoplasmic peroxide stress protein YaaA. In *E. coli*, YaaA expression is controlled by the oxidative stress-dependent OxyR response regulator. Like Cu, iron (Fe) is able to trigger hydrogen peroxide (H_2O_2) formation through a Fenton reaction. To limit Fe-induced oxidative stress, YaaA is thought to decrease the level of unincorporated Fe by reducing Fe import or increasing efflux (Liu et al. 2011). Unlike *E. coli*, the disruption of *C. crescentus yaaA* gene did not affect growth in absence of oxidative stress. However, growth is impacted under moderated Cu stress (150 μM). Since Cu also leads to oxidative stress (Osman & Cavet 2008), this stress could be exacerbated by the unincorporated Fe ions which are notably oxidized by H_2O_2 and can lead to superoxide anion formation. Decreasing Fe cytoplasmic concentration could limit oxidative stress-induced damages. This hypothesis could explain the observed sensitivity to Cu of candidate 38_8.

A phenotype similar to 38_8 was observed in 78_20 and 108_1 mutants (**, $p \leq 0.01$; ***, $p \leq 0.001$ using T-test; $N_{WT} = 40$; $N_{78_25} = 6$; $N_{108_1} = 6$) (Fig. 23A and 23B), where CCNA_03282 gene encoding a pirin has been disrupted by the transposon. Using BLAST and protein domain classification (Camacho et al. 2009; Marchler-Bauer et al. 2017), the protein has been found to be part of the YhaK pirin superfamily. YhaK was first described in *E. coli* where it could play a role in cellular redox regulation and/or in oxidative stress sensing. Among the 3 cysteines involved in redox status sensing, 2 of them are forming a disulphide bond, whereas the third one is reduced in presence of ROS (Gurmu et al. 2009). However, *C. crescentus* YhaK is devoid of cysteine (Caspi et al. 2016). The tyrosines, tryptophans and glycines present in *C. crescentus* YhaK could also be reduced although protein alignment did not show the presence of such reducible residues instead of the cysteine residues (Notredame et al. 2000).

As previously explained, Cu ions leads to the formation of ROS *in vitro* and it is thought that this metal has the same properties *in vivo* even if it is not yet proven (Osman & Cavet 2008). On the other side, the signal leading to Cu negative chemotaxis in *C. crescentus* is still unknown and it is believed that Cu ions could directly interact with one or several MCP(s) (G. Louis, personal communication). The growth and the chemotaxis ability of the 38_8, 78_20 and 108_1 mutants were affected by Cu. The 2 genes disrupted by transposition were both implicated in redox status or oxidative stress sensing. These observations could suggest a link between redox sensing and Cu chemotaxis since YaaA and YhaK are activated by oxidative stress. They induce an appropriate response, which could consist in negative chemotaxis by interacting with a MCP involved in redox status sensing, such as Tsr from *E. coli* or BdlA found in *Pseudomonas aeruginosa* (Ortega et al. 2017).

Conclusion and perspectives

Our *in silico* analysis suggested that CheAI is the main histidine kinase involved in chemotaxis since CheAII protein structure is unusual due to the absence of any P2 domain and the presence of a second P5 domain. Another observation leading to the same conclusion is the conservation of *cheAII* operon organization as this operon appeared to be specific to α -proteobacteria. On the contrary, *cheAI* operon architecture seemed more widely conserved throughout Proteobacteria. To experimentally confirm the potential role of each protein in chemotaxis, *cheAI/II* genes were deleted to construct single and double knock-out strains. It appeared that these genes had no impact on growth in absence and presence of increasing Cu concentrations. However, the $\Delta cheAI$ and $\Delta cheAI/II$ strains were not able to flee Cu. This observation reinforces bioinformatic analysis. Concerning $\Delta cheAII$, this strain showed a similar negative chemotaxis response to Cu than the WT strain.

Unlike CheAI that is thought to have an important role in chemotaxis signalling, little is known about CheAII participation in chemotaxis. Localizing this protein within the cytoplasm could determine whether CheAII is part of the cytoplasmic or in the membrane-embedded chemotaxis arrays. This could be performed by fusing this protein with a fluorescent protein such as GFP. To control that CheAII is interacting with MCP, one could imagine colocalizing membrane and cytoplasmic MCP with the histidine kinase. In addition, the presence of 2 CheA proteins could lead to homo- or heterodimer formation. To test this hypothesis, a Western blot under native conditions with a DTT control could be performed. Since native conditions do not denature dimers, the band of interest should have a molecular weight of two monomers, i.e. a CheA protein. To differentiate each protein, they should be differentially tagged with his- and Strep-tags for example. On the other side, using the same tags, co-immunoprecipitation could be performed followed by Western blot analysis. For example, if CheAI immunoprecipitates CheAII, one could expect that these 2 proteins are interacting and possibly forming heterodimers.

Even if the screening did not reach saturation (i.e. all genes involved in impaired Cu chemotaxis are uncovered), some isolated candidates showed interesting phenotypes such as non-motile strains or impaired Cu-induced chemotaxis. Interestingly, the disruption of a gene involved in oxidative stress sensing led to a reduced Cu flight. As Cu is thought to trigger formation of ROS, one could hypothesize that Cu-induced oxidative stress is sensed by the bacteria rather than Cu directly. To test this hypothesis, different approaches can be used. The first one would consist in testing the chemotaxis ability to other metal ions inducing (iron, silver) or not (magnesium) oxidative stress. Moreover, one could imagine a live chemotaxis system where the tested substance would be an oxidant such as H₂O₂.

Table 1. Strains and plasmids list.

Strains	Description
<i>C. crescentus</i>	
WT	Synchronizable variant strain of CB15
$\Delta cheAI$	Knock-out strain for <i>cheAI</i> gene
$\Delta cheAII$	Knock-out strain for <i>cheAII</i> gene
$\Delta cheAI/II$	Knock-out strain for <i>cheAI</i> and <i>cheAII</i> genes
$\Delta cheAII/pcheAII$	Knock-out strain for <i>cheAII</i> gene carrying a copy of <i>cheAII</i> on the pMR10 under control of the <i>lac</i> promoter; <i>Kan^R</i>
<i>E. coli</i>	
S17-1	RP4-2, <i>Tc::Mu</i> , <i>KM-T</i> ,7, for plasmid mobilization
Plasmids	Description
pNPTS138	mobRP4+ ori-R6K sacB; integrative vector in <i>C. crescentus</i> for in-frame deletions; <i>Kan^R</i>
pMR10	Low copy number replicative cloning vector in <i>E. coli</i> and <i>C. crescentus</i> ; <i>Kan^R</i>

Experimental procedures

I. Strains, plasmids and growth conditions

Caulobacter crescentus NA1000 was grown at 30°C PYE rich medium (0.2 % peptone, 0.1 % yeast extract, 0.8 mM MgSO₄, 0.5 mM CaCl₂) (Ely 1991) with 5 µg/ml kanamycin and/or CuSO₄·5H₂O when required. Exponentially growing cultures were used for all experiments. When necessary, swarmer (SW) cells were isolated by centrifugation using Ludox density gradient as described by Evinger and Agabian (Evinger & Agabian 1977). Synchronous SW cells were then suspended in PYE culture medium (30°C) with Cu when appropriate.

Plasmids were mobilized from *E. coli* strain S17-1 into *C. crescentus* by conjugation (Ely 1991). *E. coli* strains were cultured in Luria-Bertani broth medium. Following antibiotics concentration were used: ampicillin (100 µg/ml), kanamycin (5 µg/ml) and nalidixic acid (25 µg/ml). Strains and plasmids are listed in Table 2 and the strategies for their construction are described below.

A. Knock-out strain construction

One gBlock® Gene Fragment (Integrated DNA Technologies) was designed for each gene (*cheAI* and *cheAII*). It contains 200 upstream bp, the last 50 bp of the gene and 250 downstream bp. These gBlock® were subcloned in an *EcoRV*-linearized pNTPS138 plasmid. The ligation product was transformed into DH10B *E. coli* strain. A tri-parental mating between the DH10B *E. coli* strain containing the pNTPS138-gBlock®-*cheAI/II*, an *E. coli* Helper strain and the wild-type strain of *C. crescentus* (CB15N) was performed.

As the pNPTS vector carries genes coding for kanamycin resistance, clones which integrated the plasmid by homologous recombination were selected on a kanamycin-containing medium. Selection for a second homologous recombination event was carried out by growing kanamycin-resistant clones in PYE, under nonselective conditions and then plating these bacteria on PYE-3% sucrose plates. This process selects for the plasmid loss and creates either a knock-out *cheAI/II* strain or a wild-type (WT) strain. A final diagnostic PCR (hybridization of chromosomal DNA, 700 bp from either side of *cheA* genes) was performed to determine the genotype of each clone.

Same strategy was used to construct double *cheAI/II* knock-out strain.

B. Complementation

Concerning *cheAI* gene, a gBlock® Gene Fragment containing the first 1300 bp was used as this part could not be amplified by PCR. In contrast, the last 1000 bp could be amplified by PCR. The 2 halves were connected by a *SphI* restriction site constitutively present in *cheAI* gene. The 2 DNA fragments were restricted in respect with *SphI* and inserted into an *EcoRV*-linearized pGEM®-T plasmid. The insert was then excised using *HindIII* and *XbaI* and ligated into a low copy replicative pMR10 plasmid restricted with the same enzymes. *Via* a triparental mating, the resulting plasmid was then introduced into the CB15N strain. Clones containing pMR10-*cheAI* were checked by diagnostic PCR (hybridization on the plasmid, from either side of the insert).

cheAII sequence was amplified from *C. crescentus* genomic DNA. The PCR product was inserted into an *EcoRV*-linearized pGEM®-T plasmid. The insert was then excised using *XbaI* and *KpnI* and ligated into a low copy replicative pMR10 plasmid restricted with the same enzymes. *Via* a triparental mating, the resulting plasmid was then introduced into the CB15N

strain. Clones containing pMR10-*cheAII* were checked by diagnostic PCR (hybridization on the plasmid, from either side of the insert).

II. Growth curve measurements

Bacterial cultures (triplicates for each condition) in exponential growth phase were diluted in PYE medium to a final O.D._{660nm} of 0.05 and inoculated in 96-well plates. Bacteria were then grown for 24 h at 30°C under continuous shaking in a BioTek Epoch 2 microplate spectrophotometer where O.D._{660nm} was measured every 10 min. Different CuSO₄·5H₂O concentrations were added when appropriate

III. DNA quantification by flow cytometry

Exponentially growing cells were fixed with cold 70% (vol/vol) ethanol as previously described (Winzeler & Shapiro 1995). Fixed cells were incubated for 30 min in FACS staining buffer pH 7.2 (10 mM Tris-HCl pH 6.8, 1 mM EDTA, 50 mM NaCitrate and 0.01% TritonX-100) supplemented with 20 mg/ml of RnaseA. DNA was then labeled by washing the cells in FACS staining buffer pH 7.2 supplemented with 0.2 μM Sytox Green (Life 120 Technologies). Labeled cells were analyzed on a BD FACSCalibur flow cytometer. The data were analyzed with the CellQuest Pro software. 5.10⁴ bacteria are analyzed for each condition.

IV. Gene expression quantification

A. RNA extraction and retro-transcription

1. Extraction

A 15 mL liquid culture at a minimal O.D._{660 nm} of 0.300 was centrifuged for 10 min at 8000 RPM, 4 °C. The pellet was washed twice with cold sterile PBS to eliminate salts. The cell pellet was resuspended in 100 μL of 10 % SDS and 20 μL of proteinase K. It was then incubated for 1h at 37 °C under agitation.

From this step to the reverse transcription, it was primordial to destroy and to inhibit RNase from the samples. In this purpose, the bench and the instruments were treated with RNase ERASE.

The cell lysate was transferred in a RNase Free tube and 1 mL of TriPure Isolation Reagent was added. It was mixed thoroughly and it was then incubated for 10 min at 65°C under agitation. 200 μL of phenolchloroform was added to each sample and each tube was homogenised by reversal movements. Samples were incubated for 10 min at RT. Samples were then centrifuged for 15 min at 12 000 RPM, 4°C (Eppendorf Centrifuge 5417R). 400 μL of the sample aqueous phase were collected as it contains the RNA and it was transferred in new RNase Free tubes. 500 μL of isopropanol was added and samples were homogenised by reversal movements. They were incubated for 10 min at RT. From this step, samples could be stocked at -20 °C for few days.

2. RNA traitement

Samples were centrifuged for 30 min at 14 000 RPM, 4 °C. A RNA pellet was visible. This RNA pellet was washed twice with ethanol 70 % RNase Free and centrifuged for 5 min at 8500 RPM, 4 °C. Finally, the whole supernatant was discard and the pellets were dried out until the complete ethanol evaporation. The RNA pellet was suspended in 50 μL of DEPC H₂O and incubated for 10 min at 55 °C. The RNA concentration of each sample was measured by absorbance measurement.

3. DNase traitement

The samples were diluted to obtain a RNA concentration around 300 ng/μL. In new RNase Free tubes, the following mix was prepared:

RNA	Equivalent volume to 2 ng	Example	7 μL
Buffer 10X	1/10 of final volume		2 μL
DNaseI (1 U/μL) (Thermo Scientific)	1 μL/μg RNA		2 μL
H ₂ O DEPC	Up to final volume		9 μL
TOTAL			20 μL

The tubes were incubated for 30 min at 37 °C. 1/10 of final volume of EDTA 50 mM was added (2 μL) and samples were incubated for 10 min at 65 °C.

4. Reverse transcription

For each condition, 2 RNase Free tubes were prepared with 10 μL of DNase I-treated RNA and the following mix:

Reagents	RT +	RT -
RNA	10 μL	10 μL
Hexamer random primer 10X	2 μL	0 μL
H ₂ O RNase FREE	1.5 μL	3.5 μL

- 10 min at 65 °C'
- 5' on ice

RT Buffer 5X	4 μL	4 μL
dNTPs	2 μL	2 μL
SS II RT (Thermo Scientific)	0.5 μL	0 μL

- 10 min at 25 °C
- 45 min at 55 °C
- 5 min at 85°C

The obtained cDNA were diluted 10x and stocked at -20 °C.

B. RT-qPCR

qRT PCR were performed on the LightCycler 96 Real-Time PCR system by Roche. For each gene, the following master mix was prepared (10 μL/well):

- cDNA: 3 μL
- Primer F (900 μM): 1 μL
- Primer R (900 μM): 1 μL
- SYBR green: 5 μL

Analysis

For each condition, the ΔCt (cycle threshold) was calculated by subtracting the Ct number of the reference sample (housekeeping gene) from the target sample (gene of interest). To compare the expression change of one gene between the conditions treated and control, the Equation 1 was employed:

$$Ratio = 2^{\Delta C t_{treated} - \Delta C t_{control}} \quad \text{Equation 1.}$$

V. Live chemotaxis imaging

The live chemotaxis imaging was adapted from the “plug assay” designed in Emonet’s lab (Yale University, New Haven, USA (personal communication)). Briefly, chemotaxis devices (Fig. 17) were made by casting solubilized 10:1 polydimethylsiloxane (PDMS Sylgard 184, Dow Corning) in a small glass pot (d = 50 mm; h = 30 mm; glassware from Lenz laborglass instrument) where coverslips had been previously placed in order to mold the future bacterial chambers. After a degazing phase, the mixed PDMS was heated for 1 h at 70°C. Unmolded PDMS devices were then mounted on a microscopy glass slide. The slide and the PDMS cube were washed successively with acetone (only the slide), isopropanol, and methanol, and rinsed with milli-Q H₂O. Both components were blown dry between each wash. Three inlets and one outlet channels were drilled in the PDMS, which was then firmly pressed against the slide to seal the device. Ten µL of melted 1.5% agarose H₂O with or without 1.16 mM Cu were loaded into the chamber through both external inlet channels to generate the plugs. One hundred and fifty µL of isolated SW cells (O.D._{660nm} 0.01) were in turn injected into the bacterial chamber through the central inlet channel.

Images were collected every min for 25 min in one focal plan (near the liquid surface) in the vicinity of the Cu or the control plug with an Eclipse Ti2 inverted microscope equipped with a Nikon 20X/0.5 Ph2 objective equipped with a Hamamastu C13440 digital camera. All image capture and processing was performed with the NIS-Elements AR (blue version). Quantitative analysis of the time-lapse images was performed with MATLAB software (MathWorks).

VI. Chemotaxis mutant screening

A. Transpositional mutagenesis

A transpositional mutant library was created by inserting the mini-Tn5 (*Kan^R*) transposon into the CB15N strain. 50 µL of *E. coli* transposon carrier strain overnight culture was mixed with 950 µL of CB15N overnight culture. After a centrifugation of 2 min at 9000 rpm, the supernatant was discarded and 1 mL of PYE was added. A second 2 min centrifugation at 9000 rpm was performed. Except for 50 µL, the supernatant was discarded and the pellet was suspended in the 50 µL left supernatant. Bacteria were then dropped on PYE plate and incubated overnight at 30 °C. The drop was then mixed in 2 mL PYE and plated on PYE-Nal-Kan medium before incubation for 48 h at 30 °C. Chemotaxis-deficient mutants were selected with the chemotaxis assay.

B. Chemotaxis assay

PYE swarming medium (0.25% agar) was plated in a Petri dish containing a PYE 1.5 % agar plug (1.5 cm diameter) in the center (Fig. 12). This plug was supplemented with CuSO₄·5H₂O 5 mM when required. This concentration has been arbitrarily determined during the development of this assay. Bacteria were inoculated from either liquid culture or plates at 2 cm from the plug and were incubated for 48 h at 30°C. The swarming colonies were then imaged and the inner radius and external radius were measured via ImageJ (Schneider et al. 2012). The ratio between the inner radius and the external radius was then calculated and compared with WT. In presence of Cu, the ratio should decrease as bacteria are fleeing Cu stress (Fig 13). However, a strain with defective Cu negative chemotaxis should have a higher ratio compared to the WT strain.

C. Semi-arbitrary PCR

Mini-Tn5 insertions can be determined by a two-steps semi arbitrarily-primed PCR. The first step consists to use a specific primer (P1) hybridizing at one extremity of the Mini-Tn5 element together with a mix of 3 degenerated primers (P2, P3 and P4). The second step uses 2 specific

Table 3. Primer list.

Primer name	5' → 3' primer sequence
P1	GATCCTCTAGAGTCGACCTG
P2	GGCCACGCGTCGACTAGTACNNNNNNNNNNACGCC
P3	GGCCACGCGTCGACTAGTACNNNNNNNNNNCCTGG
P4	GGCCACGCGTCGACTAGTACNNNNNNNNNNCCTCG
P5	TGCAAGCTTCGGCCGCCTAG
P6	GGCCACGCGTCGACTAGTAC

primers (P5 and P6) hybridizing inside the first amplified sequence. Primers are listed in Table 3.

1. PCR 1

The PCR mix contained GoTaq[®] DNA polymerase (5 U/ μ L, Promega), Green GoTaq[®] Reaction Buffer (5X, Promega), dNTPs (2.5 mM each), milliQ H₂O (milliQ purification system, Millipore), and forward primer P1, and reverse primer, P2, P3 or P4 (10 μ M each) for a final volume of 50 μ L. One μ L from overnight culture was used as DNA template. The PCR 1 program was the following:

94 °C	3'	
94 °C	30''] 6x
42 °C (slope -1 °C/cycle)	30''	
72 °C	1'	
94 °C	30''] 30x
58 °C	30''	
72 °C	1'	
72 °C	10'	

2. PCR 2

The mix of this PCR differ from the previous one by the employed primers: P5 and P6. One μ L from previous PCR was used as template to amplify insertion site of the transposon. The amplification program is the next one:

94 °C	3'	
94 °C	30''] 30x
64 °C	30''	
72 °C	1'	
72 °C	10'	

3. Purification of PCR product and sequencing

Purification was achieved by using the NucleoSpin, Gel and PCR Clean-up kit (Macherey-Nagel) according to manufacturer instructions. After purification, sequencing was performed by Eurofins Europe.

Bibliography

- Alley, M.R.K., Maddock, J.R. & Shapiro, L., 1992. Polar localization of a bacterial chemoreceptor. *Genes and Development*, 6(5), pp.825–836.
- Alvarado, A. et al., 2017. Coupling chemosensory array formation and localization. *eLife*, 6.
- Argüello, J.M., Raimunda, D. & Padilla-Benavides, T., 2013. Mechanisms of copper homeostasis in bacteria. *Frontiers in Cellular and Infection Microbiology*, 3(November), pp.1–14.
- Barak, R. et al., 2006. The Chemotaxis Response Regulator CheY Can Catalyze its Own Acetylation. *Journal of Molecular Biology*, 359(2), pp.251–265.
- Barak, R. & Eisenbach, M., 2001. Acetylation of the response regulator, CheY, is involved in bacterial chemotaxis. *Molecular Microbiology*, 40(3), pp.731–743.
- Barkai, N. & Leibler, S., 1997. Robustness in simple biochemical networks to transfer and process information. *Nature*, 387(6636), pp.913–917.
- Berleman, J.E. et al., 2008. Predataxis behavior in *Myxococcus xanthus*. *Proceedings of the National Academy of Sciences*, 105(44), pp.17127–17132.
- Bhatnagar, J. et al., 2010. Structure of the ternary complex formed by a chemotaxis receptor signaling domain, the CheA histidine kinase, and the coupling protein CheW As determined by pulsed dipolar ESR spectroscopy. *Biochemistry*, 49(18), pp.3824–3841.
- Bilwes, A.M. et al., 1999. Structure of CheA, a signal-transducing histidine kinase. *Cell*, 96(1), pp.131–141.
- Bondarczuk, K. & Piotrowska-Seget, Z., 2013. Molecular basis of active copper resistance mechanisms in Gram-negative bacteria. *Cell Biology and Toxicology*, 29(6), pp.397–405.
- Bourret, R.B., Hess, J.F. & Simon, M.I., 1990. Conserved aspartate residues and phosphorylation in signal transduction by the chemotaxis protein CheY. *Proceedings of the National Academy of Sciences*, 87(January), pp.41–45.
- Bren, A. & Eisenbach, M., 1998. The N terminus of the flagellar switch protein, FliM, is the binding domain for the chemotactic response regulator, CheY. *Journal of Molecular Biology*, 278(3), pp.507–14.
- Briegel, A. et al., 2012. Bacterial chemoreceptor arrays are hexagonally packed trimers of receptor dimers networked by rings of kinase and coupling proteins. *Proceedings of the National Academy of Sciences*, 109(10), pp.3766–3771.
- Briegel, A. et al., 2008. Location and architecture of the *Caulobacter crescentus* chemoreceptor array. *Molecular Microbiology*, 69(1), pp.30–41.
- Camacho, C. et al., 2009. BLAST+: architecture and applications. *BMC Bioinformatics*, 10(1), p.421.
- Caspi, R. et al., 2016. The MetaCyc database of metabolic pathways and enzymes and the BioCyc collection of pathway/genome databases. *Nucleic Acids Research*, 44(D1), pp.D471–D480.
- Chou, W.K. et al., 2005. Identification and characterization of NeuB3 from *Campylobacter jejuni* as a pseudaminic acid synthase. *Journal of Biological Chemistry*, 280(43), pp.35922–35928.
- Curtis, P.D. & Brun, Y. V., 2010. Getting in the Loop: Regulation of Development in *Caulobacter crescentus*. *Microbiology and Molecular Biology Reviews*, 74(1), pp.13–41.
- Cuthbertson, L. & Nodwell, J.R., 2013. The TetR Family of Regulators. *Microbiology and Molecular Biology Reviews*, 77(3), pp.440–475.

- Drozdetskiy, A. et al., 2015. JPred4: A protein secondary structure prediction server. *Nucleic Acids Research*, 43(W1), pp.W389–W394.
- Ely, B., 1991. Genetics of *Caulobacter crescentus*. *Methods in Enzymology*, 204, pp.372–384.
- Endres, R.G. & Wingreen, N.S., 2006. Precise adaptation in bacterial chemotaxis through “assistance neighborhoods”. *Proceedings of the National Academy of Sciences*, 103(35), pp.13040–13044.
- Evinger, M. & Agabian, N., 1977. Envelope-associated nucleoid from *Caulobacter crescentus* stalked and swarmer cells. *Journal of Bacteriology*, 132(1), pp.294–301.
- Flemming, H.-C. et al., 2016. Biofilms: an emergent form of bacterial life. *Nature Reviews Microbiology*, 14(9), pp.563–575.
- Gestwicki, J.E. et al., 2000. Evolutionary Conservation of Methyl-Accepting Chemotaxis Protein Location in Bacteria and Archaea. *Journal of Bacteriology*, 182(22), pp.6499–6502.
- Gomes, S.L. & Shapiro, L., 1984. Differential expression and positioning of chemotaxis methylation proteins in *Caulobacter*. *Journal of Molecular Biology*, 178(3), pp.551–568.
- Gurmu, D. et al., 2009. The crystal structure of the protein YhaK from *Escherichia coli* reveals a new subclass of redox sensitive enterobacterial bicupins. *Proteins: Structure, Function and Bioinformatics*, 74(1), pp.18–31.
- Hess, J.F. et al., 1988. Phosphorylation of three proteins in the signaling pathway of bacterial chemotaxis. *Cell*, 53(1), pp.79–87.
- Higgins, D. & Dworkin, J., 2012. Recent progress in *Bacillus subtilis* sporulation. *FEMS Microbiology Reviews*, 36(1), pp.131–148.
- Hughes, K.T. & Berg, H.C., 2017. The bacterium has landed. *Science*, 358(6362), pp.446–447.
- Huitema, E. et al., 2006. Bacterial birth scar proteins mark future flagellum assembly site. *Cell*, 124(5), pp.1025–1037.
- Irving, H. & Williams, R.J.P., 1953. The Stability of Transition-metal Complexes. *J. Chem Soc.*, 0(3192–3210).
- Jahreis, K. et al., 2004. Chemotactic Signaling by an *Escherichia coli* CheA Mutant That Lacks the Binding Domain for Phosphoacceptor Partners. *Journal of Bacteriology*, 186(9), pp.2664–2672.
- Jones, C.W. & Armitage, J.P., 2015. Positioning of bacterial chemoreceptors. *Trends in Microbiology*, 23(5), pp.1–10.
- Jourand, P. et al., 2004. *Methylobacterium nodulans* sp. nov., for a group of aerobic, facultatively methylotrophic, legume root-nodule-forming and nitrogen-fixing bacteria. *International Journal of Systematic and Evolutionary Microbiology*, 54(6), pp.2269–2273.
- Kentner, D. & Sourjik, V., 2009. Dynamic map of protein interactions in the *Escherichia coli* chemotaxis pathway. *Molecular Systems Biology*, 5(238).
- Khursigara, C.M. et al., 2008. Role of HAMP domains in chemotaxis signaling by bacterial chemoreceptors. *Proceedings of the National Academy of Sciences*, 105(43), pp.16555–60.
- Kimura, T. & Nishioka, H., 1997. Intracellular generation of superoxide by copper sulphate in *Escherichia coli*. *Mutation Research - Genetic Toxicology and Environmental Mutagenesis*, 389(2–3), pp.237–242.
- Kumar, K., Mella-Herrera, R.A. & Golden, J.W., 2010. Cyanobacterial Heterocysts. *Cold Spring Harbor Perspectives in Biology*, 2(315), pp.1–19.
- Lacal, J. et al., 2010. Sensing of environmental signals: Classification of chemoreceptors according to

- the size of their ligand binding regions. *Environmental Microbiology*, 12(11), pp.2873–2884.
- Ladomersky, E. & Petris, M.J., 2015. Copper tolerance and virulence in bacteria. *Metallomics*, 7(6), pp.957–964.
- Lai, R.Z. & Parkinson, J.S., 2014. Functional suppression of HAMP domain signaling defects in the E. Coli serine chemoreceptor. *Journal of Molecular Biology*, 426(21), pp.3642–3655.
- Laub, M.T., Shapiro, L. & McAdams, H.H., 2007. Systems Biology of Caulobacter. *Annual Review of Genetics*, 41(1), pp.429–441.
- Lawarée, E. et al., 2016. Caulobacter crescentus intrinsic dimorphism provides a prompt bimodal response to copper stress. *Nature Microbiology*, 1, pp.1–7.
- Levit, M.N., Liu, Y. & Stock, J.B., 1999. Mechanism of CheA Protein Kinase Activation in Receptor Signaling Complexes. *Biochemistry*, 38(20), pp.6651–6658.
- Li, R. et al., 2010. CobB regulates Escherichia coli chemotaxis by deacetylating the response regulator CheY. *Molecular Microbiology*, 76(5), pp.1162–1174.
- Li, Y. et al., 2007. Solution structure of the bacterial chemotaxis adaptor protein CheW from Escherichia coli. *Biochemical and Biophysical Research Communications*, 360(4), pp.863–867.
- Liarzi, O. et al., 2010. Acetylation represses the binding of CheY to its target proteins. *Molecular Microbiology*, 76(4), pp.932–943.
- Liu, Y., Bauer, S.C. & Imlay, J.A., 2011. The YaaA protein of the Escherichia coli OxyR regulon lessens hydrogen peroxide toxicity by diminishing the amount of intracellular unincorporated iron. *Journal of Bacteriology*, 193(9), pp.2186–2196.
- Marchler-Bauer, A. et al., 2017. CDD/SPARCLE: Functional classification of proteins via subfamily domain architectures. *Nucleic Acids Research*, 45(D1), pp.D200–D203.
- McEvoy, M.M. et al., 1996. Structure and dynamics of a CheY-binding domain of the chemotaxis kinase CheA determined by nuclear magnetic resonance spectroscopy. *Biochemistry*, 35(18), pp.5633–5640.
- Meir, Y. et al., 2010. Precision and kinetics of adaptation in bacterial chemotaxis. *Biophysical Journal*, 99(9), pp.2766–2774.
- Mercier, R. & Mignot, T., 2016. Regulations governing the multicellular lifestyle of Myxococcus xanthus. *Current Opinion in Microbiology*, 34, pp.104–110.
- Mermod, M. et al., 2012. The copper-inducible ComR (YcfQ) repressor regulates expression of ComC (YcfR), which affects copper permeability of the outer membrane of Escherichia coli. *BioMetals*, 25(1), pp.33–43.
- Mo, G. et al., 2012. Solution structure of a complex of the histidine auto kinase CheA with its substrate CheY. *Biochemistry*, 51(18), pp.3786–3798.
- Morse, M. et al., 2015. Flagellar Motor Switching in Caulobacter Crescentus Obeys First Passage Time Statistics. *Physical Review Letters*, 115(19), pp.1–5.
- Mourey, L. et al., 2001. Crystal Structure of the CheA Histidine Phosphotransfer Domain that Mediates Response Regulator Phosphorylation in Bacterial Chemotaxis. *Journal of Biological Chemistry*, 276(33), pp.31074–31082.
- Nathan, P. et al., 1986. Differential localization of membrane receptor chemotaxis proteins in the Caulobacter predivisional cell. *Journal of Molecular Biology*, 191(3), pp.433–440.
- Nesper, J. et al., 2017. Cyclic di-GMP differentially tunes a bacterial flagellar motor through a novel class of CheY-like regulators. *eLife*, 6, pp.1–25.

- Nierman, W.C. et al., 2001. Complete genome sequence of *Caulobacter crescentus*. *Proceedings of the National Academy of Sciences*, 98(7), pp.4136–4141.
- Nishiyama, S.I., Garzón, A. & Parkinson, J.S., 2014. Mutational analysis of the P1 phosphorylation domain in *Escherichia coli* CheA, the signaling kinase for chemotaxis. *Journal of Bacteriology*, 196(2), pp.257–264.
- Notredame, C., Higgins, D.G. & Heringa, J., 2000. T-coffee: a novel method for fast and accurate multiple sequence alignment. *Journal of Molecular Biology*, 302(1), pp.205–217.
- Ordax, M. et al., 2010. Exopolysaccharides favor the survival of *Erwinia amylovora* under copper stress through different strategies. *Research in Microbiology*, 161(7), pp.549–555.
- Ortega, A., Zhulin, I.B. & Krell, T., 2017. Sensory Repertoire of Bacterial Chemoreceptors. *Microbiology and Molecular Biology Reviews*, 81(4), pp.1–28.
- Osman, D. & Cavet, J.S., 2008. Copper Homeostasis in Bacteria. *Advances in Applied Microbiology*, 65(8), pp.217–247.
- Paredes-Sabja, D., Shen, A. & Sorg, J.A., 2014. *Clostridium difficile* spore biology: Sporulation, germination, and spore structural proteins. *Trends in Microbiology*, 22(7), pp.406–416.
- Parkinson, J.S., Hazelbauer, G.L. & Falke, J.J., 2015. Signaling and sensory adaptation in *Escherichia coli* chemoreceptors: 2015 update. *Trends in Microbiology*, 23(5), pp.257–266.
- Porter, S.L. & Armitage, J.P., 2004. Chemotaxis in *Rhodobacter sphaeroides* requires an atypical histidine protein kinase. *Journal of Biological Chemistry*, 279(52), pp.54573–54580.
- Porter, S.L., Wadhams, G.H. & Armitage, J.P., 2008. *Rhodobacter sphaeroides*: complexity in chemotactic signalling. *Trends in Microbiology*, 16(6), pp.251–260.
- Porter, S.L., Wadhams, G.H. & Armitage, J.P., 2011. Signal processing in complex chemotaxis pathways. *Nature Reviews Microbiology*, 9(3), pp.153–165.
- Rensing, C. & Grass, G., 2003. *Escherichia coli* mechanisms of copper homeostasis in a changing environment. *FEMS Microbiology Reviews*, 27(2–3), pp.197–213.
- Salah Ud-Din, A.I.M. & Roujeinikova, A., 2017. Methyl-accepting chemotaxis proteins: a core sensing element in prokaryotes and archaea. *Cellular and Molecular Life Sciences*, 0(0), pp.1–11.
- Schneider, C.A., Rasband, W.S. & Eliceiri, K.W., 2012. NIH Image to ImageJ: 25 years of image analysis. *Nature Methods*, 9(7), pp.671–675.
- Schrader, J.M. et al., 2016. Dynamic translation regulation in *Caulobacter* cell cycle control. *Proceedings of the National Academy of Sciences*, 113(44), pp.E6859–E6867.
- Schulmeister, S. et al., 2008. Protein exchange dynamics at chemoreceptor clusters in *Escherichia coli*. *Proceedings of the National Academy of Sciences*, 105(17), p.6403.
- Segall, J.E., Block, S.M. & Berg, H.C., 1986. Temporal comparisons in bacterial chemotaxis. *Proceedings of the National Academy of Sciences*, 83(23), pp.8987–8991.
- Shiomi, D. et al., 2006. Helical distribution of the bacterial chemoreceptor via colocalization with the Sec protein translocation machinery. *Molecular Microbiology*, 60(4), pp.894–906.
- Skerker, J.M. & Laub, M.T., 2004. Cell-cycle progression and the generation of asymmetry in *Caulobacter crescentus*. *Nature reviews. Microbiology*, 2(4), pp.325–37.
- Son, K., Guasto, J.S. & Stocker, R., 2013. Bacteria can exploit a flagellar buckling instability to change direction. *Nature Physics*, 9(8), pp.494–498.
- Taktikos, J., Stark, H. & Zaburdaev, V., 2013. How the motility pattern of bacteria affects their dispersal

- and chemotaxis. *PLoS ONE*, 8(12).
- Wadhams, G.H. & Armitage, J.P., 2004. Making sense of it all: bacterial chemotaxis. *Nature Reviews Molecular Cell Biology*, 5(12), pp.1024–1037.
- Walukiewicz, H.E. et al., 2014. Interactions among the three adaptation systems of *Bacillus subtilis* chemotaxis as revealed by an in vitro receptor-kinase assay. *Molecular Microbiology*, 93(6), pp.1104–1118.
- Wang, X. et al., 2014. The linker between the dimerization and catalytic domains of the CheA histidine kinase propagates changes in structure and dynamics that are important for enzymatic activity. *Biochemistry*, 53(5), pp.855–861.
- Webb, B. & Sali, A., 2016. Comparative Protein Structure Modeling Using MODELLER. *Current Protocols in Bioinformatics*, (June), p.5.6.1-5.6.37.
- Weis, R.M. & Koshland, D.E., 1988. Reversible receptor methylation is essential for normal chemotaxis of *Escherichia coli* in gradients of aspartic acid. *Proceedings of the National Academy of Sciences*, 85(1), pp.83–7.
- Winzeler, E. & Shapiro, L., 1995. Use of Flow cytometry to identify a *Caulobacter* 4.5 S RNA Temperature-sensitive Mutant Defective in the Cell Cycle. *Journal of Molecular Biology*, 251(3), pp.346–365.
- Wuichet, K. & Zhulin, I.B., 2010. Origins and Diversification of a Complex Signal Transduction System in Prokaryotes. *Science Signaling*, 3(128), pp.1–13.
- Xu, Y. et al., 2015. *Pseudovibrio hongkongensis* sp. nov., isolated from a marine flatworm. *Antonie van Leeuwenhoek, International Journal of General and Molecular Microbiology*, 108(1), pp.127–132.
- Yan, J. et al., 2008. In Vivo Acetylation of CheY, a Response Regulator in Chemotaxis of *Escherichia coli*. *Journal of Molecular Biology*, 376(5), pp.1260–1271.
- Yuan, J. et al., 2012. Adaptation at the output of the chemotaxis signalling pathway. *Nature*, 484(7393), pp.233–236.
- Zhao, R. et al., 2002. Structure and catalytic mechanism of the *E. coli* chemotaxis phosphatase CheZ. *Nature Structural Biology*, 9(8).
- Zusman, D.R. et al., 2007. Chemosensory pathways, motility and development in *Myxococcus xanthus*. *Nature Reviews Microbiology*, 5(11), pp.862–872.

Figure S1. CheAI secondary structure prediction via JPred4. The first line of the prediction is the query sequence, i.e. CheAI protein sequence. The domain determination was previously performed by homologies with *E. coli* and *T. maritima* CheA proteins. The second line, the conservation, displays a conservation score for each amino acid while the quality, the third line, informs the quality of the conservation prediction with above, the consensus sequence. The fifth line represent the secondary structure prediction with the prediction confidence on line 7. α helices are represented in red, β sheets in green. Conserved histidine autophosphorylation site is exhibited in (a) while the ATP-binding pocket is highlighted in (b). The structure prediction is consistent with CheA structural models and, therefore, CheAI seems to have a classic CheA structure (Bilwes et al. 1999; Drozdetskiy et al. 2015; McEvoy et al. 1996; Mourey et al. 2001).

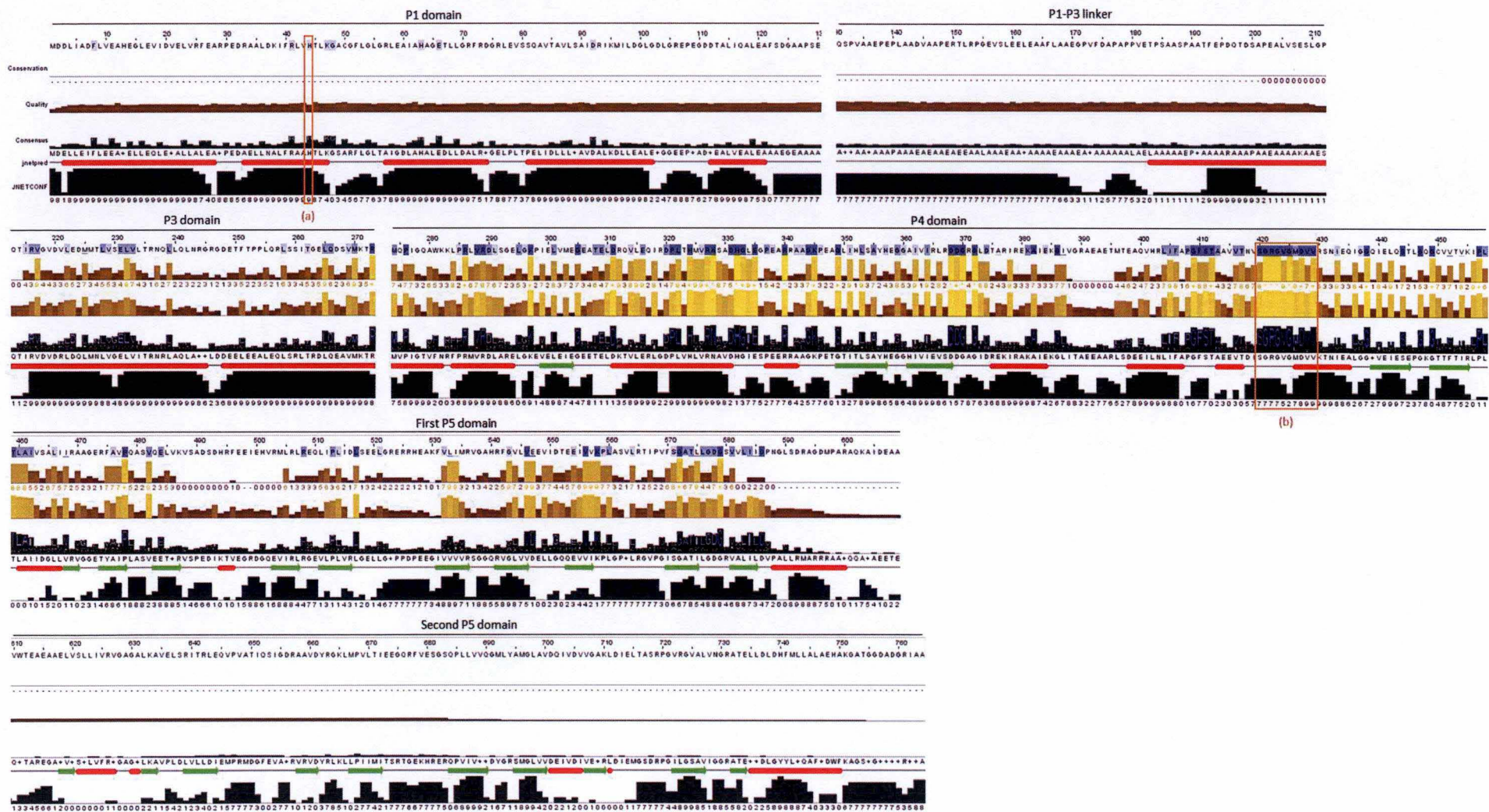


Figure S2. CB15N CheAII secondary structure prediction via JPred4. The first line of the prediction is the query sequence, i.e. CheAII protein sequence. The domain determination was previously performed by homologies with *E. coli* and *T. maritima* CheA proteins. The second line, the conservation, displays a conservation score for each amino acid while the quality, the third line, informs the quality of the conservation prediction with above, the consensus sequence. The fifth line represents the secondary structure prediction with the prediction confidence on line 7. α helices are represented in red, β sheets in green. Conserved histidine autophosphorylation site is exhibited in (a) while the ATP-binding pocket is highlighted in (b). The secondary structure prediction highlighted two important differences in CheAII compared to CheA models. The first one is the absence of any structure in the region between the P1 and the P3 domains. This observation could suggest the absence of any P2 domain. In addition, homologies predicted the presence of a second P5 domain in C-terminus. In the hypothetical secondary P5 domain region, a structure pattern seems to be consistent with this hypothesis (Bilwes et al. 1999; Drozdetskiy et al. 2015; McEvoy et al. 1996; Mourey et al. 2001).

Table S1. Phylogeny classification of chosen organisms for synteny investigation. Number in parenthesis are the *cheA* gene number, count was based on genome annotation. Organisms selection and classification are based on phylogeny tree construction (Caspi et al. 2016; Williams et al. 2010; Williams et al. 2007; Gupta 2006; Garrity et al. 2004).

Class	Order	Species
Alphaproteobacteria	Rhizobiales	<i>Rhodopseudomonas palustris</i> (5)
		<i>Methylobacterium nodulans</i> (3)
	Rhodobacteraceae	<i>Rhodobacter sphaeroides</i> (4)
		<i>Labrenzia alba</i> (3)
		<i>Pseudovibrio hongkongensis</i> (5)
	Sphingomonadales	<i>Zymomonas mobilis</i> (2)
	Rhodospirales	<i>Rhodospirillum rubrum</i> (3)
Caulobacterales	<i>Caulobacter sp. K31</i> (3)	
Betaproteobacteria	Burkholderiales	<i>Burkholderia pseudomallei</i> (2)
Gammaproteobacteria	Vibrionales	<i>Vibrio cholerae</i> (3)
	Aeromonadales	<i>Aeromonas hydrophila</i> (2)
	Alteromonadales	<i>Alteromonadales bacterium</i> (3)
		<i>Marinobacter hydrocarbonoclasticus</i> (2)
	Pseudomonadales	<i>Pseudomonas putida</i> (3)
		<i>Pseudomonas mendocina</i> (4)
		<i>Pseudomonas aeruginosa</i> (2)
		<i>Psychrobacter cryohalolentis</i> (2)
	Oceanospirillales	<i>Hahella chejuensis</i> (6)
	Chromatiales	<i>Alkalilimnicola ehrlichei</i> (2)
<i>Halorhodospira halophila</i> (3)		
Deltaproteobacteria	Myxococcales	<i>Myxococcus xanthus</i> (4)
	Desulfuromonadales	<i>Geobacter sp.</i> (4)
Epsilonproteobacteria	Campylobacterales	<i>Wolinella succinogenes</i> (2)

Table S2 Synteny for *cheAI* operon. Previously selected organisms genomes were investigated for the presence of synteny with the *C. crescentus* genome and specially, in the region of *cheAI* operon. *cheAI* operon is annotated from *mcpA* (CCNA_00439) to *cheE* (CCNA_00450). Green colour indicates the presence of a conserved local chromosomal organisation in respect with *cheAI* operon; yellow colour means that a homologous gene is present in the examined organism but the organisation is different from *C. crescentus* genome; red colour suggests the absence of any homologous gene. The conservation of this gene seems to concern a core of some genes, from *cheY* (CCNA_00441) to *cheYIII* (CCNA_00446), with some organisms containing a homologous gene of *cheD* (CCNA_00447). This operon organisation appears to be conserved among the different proteobacteria classes (Vallenet et al. 2009; Nierman et al. 2001).

	McpA CCNA_00439	CheX CCNA_00440	CheY CCNA_00441	CheAI CCNA_00442	CheW CCNA_00443	CheR CCNA_00444	CheB CCNA_00445	CheYII CCNA_00446	CheD CCNA_00447	CheU CCNA_00448	CheYIII CCNA_00449	CheE CCNA_00450
<i>Rhodopseudomonas palustris</i>	Red	Red	Green	Green	Red	Green	Green	Yellow	Red	Red	Red	Red
<i>Methylobacterium nodulans</i>	Red	Red	Green	Green	Yellow	Green	Green	Yellow	Red	Red	Red	Red
<i>Rhodobacter sphaeroides</i>	Red	Green	Green	Green	Green	Green	Yellow	Green	Green	Red	Red	Red
<i>Labrenzia alba</i>	Red	Red	Green	Red	Red	Red	Green	Green	Red	Red	Red	Red
<i>Pseudovibrio hongkongensis</i>	Red	Red	Red	Red	Red	Red	Green	Red	Red	Red	Red	Red
<i>Zymomonas mobilis</i>	Green	Green	Green	Green	Green	Green	Green	Green	Green	Red	Red	Red
<i>Rhodospirillum rubrum</i>	Red	Red	Yellow	Yellow	Green	Yellow	Yellow	Yellow	Yellow	Red	Red	Red
<i>Caulobacter sp. K31</i>	Red	Green	Green	Green	Green	Green	Green	Green	Green	Green	Green	Green
<i>Vibrio cholerae</i>	Red	Red	Yellow	Green	Red	Yellow	Green	Green	Yellow	Red	Red	Red
<i>Aeromonas hydrophila</i>	Red	Green	Green	Green	Red	Green	Green	Green	Green	Red	Red	Red
Altermonadales bacterium	Red	Red	Green	Green	Green	Green	Green	Green	Green	Red	Red	Red
<i>Pseudomonas putida</i>	Red	Red	Green	Green	Yellow	Red	Green	Green	Red	Red	Red	Red
<i>P. mendocina</i>	Red	Red	Green	Green	Green	Green	Green	Green	Yellow	Red	Red	Red
<i>P. aeruginosa</i>	Red	Red	Green	Green	Green	Green	Green	Yellow	Green	Red	Red	Red
<i>Marinobacter Hydrocarboclasticus</i>	Red	Red	Green	Green	Red	Red	Green	Green	Red	Red	Red	Red
<i>Hahella chejuensis</i>	Green	Red	Green	Green	Green	Green	Green	Yellow	Green	Red	Red	Red
<i>Psychrobacter cryohalolentis</i>	Green	Red	Green	Red	Red	Red	Red	Red	Red	Red	Red	Red
<i>Alkalilimnicola ehrlichi</i>	Red	Red	Green	Green	Green	Green	Green	Green	Red	Red	Red	Red
<i>Halorhodospira halophila</i>	Green	Red	Green	Green	Green	Green	Green	Green	Green	Red	Red	Red
<i>Wolinella succinogenes</i>	Red	Red	Yellow	Red	Yellow	Yellow	Yellow	Yellow	Red	Red	Red	Red
<i>Myxococcus xanthus</i>	Red	Red	Yellow	Yellow	Yellow	Red	Yellow	Yellow	Red	Red	Red	Red
<i>Geobacter metallireducens</i>	Red	Yellow	Green	Yellow	Green	Green	Green	Yellow	Red	Red	Red	Red
<i>Burkholderia pseudomallei</i>	Red	Red	Green	Green	Green	Green	Green	Green	Red	Red	Red	Red

Table S3. Synteny for *cheAII* operon. Previously selected organisms genomes were investigated for the presence of synteny with the *C. crescentus* genome and specially, in the region of *cheAII* operon. *cheAII* operon is annotated from *mcpK* (CCNA_00629) to *cheRII* (CCNA_00634). Since other chemotaxis genes are also present in this region, synteny was also examined for these genes. Green colour indicates the presence of a conserved local chromosomal organisation in respect with *cheAI* operon; yellow colour means that a homologous gene is present in the examined organism but the organisation is different from *C. crescentus* genome; red colour suggests the absence of any homologous gene. The conservation of the *cheAII* operon seems to only concern alphaproteobacteria. In other proteobacteria classes, only homologous genes seem to be present and these genes organisation should be different (Vallet et al. 2009; Nierman et al. 2001).

	CheY CCNA_00625	McpG CCNA_00626	CCNA_00627	CheY CCNA_00628	McpK CCNA_00629	CheAII CCNA_00630	CheWII CCNA_00631	CheYIV CCNA_00632	CheBII CCNA_00633	ChRII CCNA_00634
<i>Rhodopseudomonas palustris</i>	Green	Green	Green	Green	Green	Green	Green	Green	Green	Green
<i>Methylobacterium nodulans</i>	Green	Green	Green	Green	Green	Green	Green	Green	Green	Green
<i>Rhodobacter sphaeroides</i>	Yellow	Yellow	Yellow	Yellow	Yellow	Yellow	Yellow	Yellow	Yellow	Yellow
<i>Labrenzia alba</i>	Green	Green	Green	Green	Green	Green	Green	Green	Green	Green
<i>Pseudovibrio hongkongensis</i>	Green	Green	Green	Green	Green	Green	Green	Green	Green	Green
<i>Zymomonas mobilis</i>	Green	Green	Green	Green	Green	Green	Green	Green	Green	Red
<i>Rhodospirillum rubrum</i>	Green	Green	Yellow	Yellow	Green	Green	Green	Green	Green	Green
<i>Caulobacter sp. K31</i>	Yellow	Yellow	Yellow	Yellow	Yellow	Yellow	Yellow	Yellow	Yellow	Yellow
<i>Vibrio cholerae</i>	Green	Green	Green	Green	Green	Green	Green	Green	Green	Yellow
<i>Aeromonas hydrophila</i>	Green	Green	Yellow	Yellow	Green	Green	Green	Green	Green	Yellow
Altermonadales bacterium	Green	Green	Green	Green	Green	Green	Green	Green	Green	Yellow
<i>Pseudomonas putida</i>	Green	Green	Green	Yellow	Green	Green	Green	Green	Green	Yellow
<i>P. mendocina</i>	Yellow	Yellow	Yellow	Yellow	Yellow	Yellow	Yellow	Yellow	Yellow	Yellow
<i>P. aeruginosa</i>	Green	Green	Green	Green	Green	Green	Green	Green	Green	Green
<i>Marinobacter Hydrocarboclasticus</i>	Green	Green	Green	Yellow	Green	Green	Green	Green	Green	Yellow
<i>Hahella chejuensis</i>	Green	Green	Green	Green	Green	Green	Green	Green	Green	Yellow
<i>Psychrobacter cryohalolentis</i>	Green	Green	Green	Green	Green	Green	Green	Green	Green	Yellow
<i>Alkalilimnicola ehrlichi</i>	Green	Green	Green	Green	Green	Green	Green	Green	Green	Yellow
<i>Halorhodospira halophila</i>	Green	Green	Green	Green	Green	Green	Green	Green	Green	Yellow
<i>Wolinella succinogenes</i>	Green	Green	Green	Green	Green	Yellow	Yellow	Yellow	Yellow	Yellow
<i>Myxococcus xanthus</i>	Yellow	Yellow	Yellow	Yellow	Yellow	Yellow	Yellow	Yellow	Yellow	Yellow
<i>Geobacter metallireducens</i>	Yellow	Yellow	Yellow	Yellow	Green	Yellow	Yellow	Green	Green	Green
<i>Burkholderia pseudomallei</i>	Green	Green	Green	Green	Green	Green	Green	Green	Green	Green